Complexes of Cobalt(II) Chloride with the Tripodal Trisphosphane triphos: Solution Dynamics, Spin-Crossover, Reactivity, and Redox Activity

Katja Heinze, Gottfried Huttner,* Laszlo Zsolnai, and Peter Schober

Department of Inorganic Chemistry, University of Heidelberg, Im Neuenheimer Feld 270, D-69120 Heidelberg, Germany

Received May 8, 1997[⊗]

Depending on the reaction conditions, different products are obtained from the reaction of $CoCl_2$ with $CH_3C(CH_2PPh_2)_3$ (triphos), including the low-spin complexes $[(triphos)Co(\mu\text{-}Cl)_2Co(triphos)]^{2+}$ ($\mathbf{1}^{2+}$) and $[(triphos)CoCl_2]$ (**3**), their solid-state structures being determined by X-ray methods. In solution, additionally, a four-coordinate high-spin complex $[(\eta^2\text{-}triphos)CoCl_2]$ (**2**) is present, its concentration relative to that of **3** depending on the solvent and the temperature. The reactivity of these species toward Lewis acids is investigated leading to the novel heterodinuclear complexes $[(triphos)Co(\mu\text{-}Cl)_2MCl_2]$ (M = Fe (**5**), Co (**6**)). Reactions with Lewis bases L yield complexes of the rare type $[(triphos)CoCl(L)]^+$ (L = CO ($\mathbf{7}^+$), PMe_3 ($\mathbf{8}^+$), NH_3 ($\mathbf{9}^+$), CH_3CN ($\mathbf{10}^+$)). One-electron reduction of **3** leads to the previously prepared pseudotetrahedral $[(triphos)Co^{I}Cl]$ complex **11**, and one-electron oxidation to the novel trigonal-bipyramidal low-spin complex $[(triphos)Co^{III}Cl_2]^+$ ($\mathbf{12}^+$).

Introduction

The reaction of triphos [1,1,1-tris((diphenylphosphino)methyl)ethane, $CH_3C(CH_2PPh_2)_3$] with $CoCl_2$ yields—depending on the reaction conditions—different products of the composition $[(triphos)CoCl_2]$ with markedly different optical and magnetic properties. As these solutions of triphos and $CoCl_2$ are of substantial synthetic utility,[1] leading e.g. to the dinuclear dinitrogen complex $[(triphos)Co(\mu\text{-}N_2)Co(triphos)]$[1a] or via $[(triphos)Co^{I}Cl]$[2] to the $[(triphos)Co^{I}(allyl)]$ complex,[1b] it was of importance to establish the nature of the species existing in these solutions. Addition of $NaBPh_4$ to the mixture yields the well-defined red complex $[(triphos)Co(\mu\text{-}Cl)_2Co(triphos)](BPh_4)_2$ ($\mathbf{1}(BPh_4)_2$) previously reported by Sacconi et al.,[3] who correctly assigned its dinuclear structure. The dinuclear arrangement is now confirmed by an X-ray structure determination (vide infra). Davis et al.[4] obtained from mixtures of triphos and $CoCl_2$ in acetone by refluxing under air a blue material which was formulated as $[(triphos)CoCl_2]$, but this material showed physical properties suggestive of the presence of phosphine oxide.[3] In order to shed some light onto this problem we have conducted experiments in different solvents and at different temperatures with rigorous exclusion of oxygen showing that in solution two monomeric isomers (**2**, **3**) undergoing a five-coordinate (**3**)/tetrahedral (**2**) interconversion exist. The red, five-coordinate isomer **3** can be isolated as a red, cystalline material, the five-coordination being confirmed by X-ray diffraction methods. As the tetrahedral isomer **2** cannot be isolated as a solid, the solid-state structure of the analogous complex $(dppp)CoCl_2$ (**4**) has been determined in order to compare bond lengths and angles with that of isomer **3**. The isomerization in solution is accompanied by a change of the spin-state of the Co^{II} ion from a doublet state ($S = {}^1/_2$) to a quartet state ($S = {}^3/_2$). The thermodynamic parameters of this equilibrium are investigated and compared to previously reported Co^{II} spin-crossover compounds.[5,23,24] The conversion of the monomeric species (**2**, **3**) into the dinuclear complex $\mathbf{1}^{2+}$ and vice versa is easily accomplished by adding chloride accepting and chloride-donating reagents, respectively.

The use of the monomeric complexes as starting materials is further demonstrated by their reaction with various Lewis acids and bases as well as their activity in redox reactions. Reaction with Lewis acids yields, depending on the acid strength and the solvent, the dinuclear complex $\mathbf{1}^{2+}$ or the novel heterodinuclear complexes **5** and **6** $[(triphos)Co(\mu\text{-}Cl)_2MCl_2]$ with one low-spin Co^{II} and one high-spin M^{II} center (M = Fe, Co) connected by two chloride bridges. The solid-state structures of both dinuclear complexes are determined by X-ray structural analyses. Chloride substitution by Lewis bases L affords complexes of the relatively rare type $[(triphos)Co^{II}Cl(L)]^+$ ($\mathbf{7}^+$−$\mathbf{10}^+$) (L = CO, PMe_3, NH_3, and CH_3CN, respectively) where two different separate coligands besides the triphos ligand are bound to the Co^{II} center. The carbonyl derivative was previously prepared by Sacconi et al. starting from the dimer complex $\mathbf{1}(BPh_4)_2$.[1g] The mechanism of the chloride substitution can either be an associative (A) or a dissociative (D) process depending on the reaction conditions and the nature of the reagent. Reduction of the monomeric complexes **2** or **3** with

⊗ Abstract published in *Advance ACS Abstracts,* November 1, 1997.

(1) (a) Cecconi, F.; Ghilardi, C. A.; Midollini, S.; Moneti, S.; Orlandini, A.; Bacci, M. *J. Chem. Soc., Chem. Commun.* **1985**, 731. (b) Sernau, V.; Huttner, G.; Scherer, J.; Zsolnai, L.; Seitz, T. *Chem. Ber.* **1995**, *128*, 193. (c) Cecconi, F.; Ghilardi, C. A.; Midollini, S.; Moneti, S.; Orlandini, A. *J. Organomet. Chem.* **1987**, *323*, C5. (d) Bianchini, C.; Masi, D.; Mealli, C.; Meli, A.; Martini, G.; Laschi, F.; Zanello, P. *Inorg. Chem.* **1987**, *26*, 3683. (e) Ghilardi, C. A.; Laschi, F.; Midollini, S.; Orlandini, A.; Scapacci, G.; Zanello, P. *J. Chem. Soc., Dalton Trans.* **1995**, 531. (f) Heinze, K.; Huttner, G.; Zsolnai, L.; Jacobi, A.; Schober, P. *Chem. Eur. J.* **1997**, *5*, 732. (g) Ghilardi, C. A.; Midollini, S.; Sacconi, L. *J. Organomet. Chem.* **1980**, *186*, 279.
(2) (a) Sacconi, L.; Midollini, S. *J. Chem. Soc., Dalton Trans.* **1972**, 1213. (b) Ellermann, J.; Schindler, J. F. *Chem. Ber.* **1976**, *109*, 1095. (c) Ellermann, J. *J. Organomet. Chem.* **1975**, *94*, 201.
(3) Mealli, C.; Midollini, S.; Sacconi, L. *Inorg. Chem.* **1975**, *14*, 2513.
(4) Davis, R.; Fergusson, J. E. *Inorg. Chim. Acta* **1970**, *4*, 23.
(5) (a) Morassi, R.; Bertini, I.; Sacconi, L. *Coord. Chem. Rev.* **1973**, *11*, 343. (b) Sacconi, L. *Pure Appl. Chem.* **1971**, *27*, 161. (c) Zarembowitch, J.; Kahn, O. *Inorg. Chem.* **1984**, *23*, 589. (d) Zarembowitch, J.; Claude, R.; Thuéry, P. *Nouv. J. Chem.* **1985**, *9*, 467. (e) Marzilli, L. G.; Marzilli, P. A. *Inorg. Chem.* **1972**, *11*, 457. (f) Murray, K. S.; Sheahan, R. M. *J. Chem. Soc., Dalton Trans.* **1976**, 999. (g) Earnshaw, A.; Hewlett, P. C.; King, E. A.; Larkworthy, L. F. *J. Chem. Soc. A* **1968**, 241. (h) Kennedy, B. J.; Fallon, G. D.; Gatehouse, B. M. K. C.; Murray, K. S. *Inorg. Chem.* **1984**, *23*, 580. (i) Nivorozhkin, A. L.; Toftlund, H.; Nielsen, M. *J. Chem. Soc., Dalton Trans.* **1994**, 361. (j) Simmons, M. G.; Wilson, L. J. *Inorg. Chem.* **1977**, *16*, 126. (k) Kremer, S.; Henke, W.; Reinen, D. *Inorg. Chem.* **1982**, *21*, 3013. (l) Sacconi, L.; Speroni, G. P. *Inorg. Chem.* **1968**, *7*, 295. (m) Sacconi, L.; Bertini, I. *Inorg. Chem.* **1968**, *7*, 1178.

S0020-1669(97)00535-1 CCC: $14.00

$NaBH_4$,[2a] BH_3·THF or NEt_3[6] yields the previously decribed pseudotetrahedral complex [(triphos)$Co^{I}Cl$] (**11**).[2] Its structure is confirmed by an X-ray structural analysis. It is proposed that the reduction process is initiated by a substitution of one chloride ion by a hydride, involving an unstable [(triphos)Co(Cl)(H)] intermediate. According to cyclovoltammetric experiments, oxidation of the [(triphos)$CoCl_2$] monomer (**3**) is also possible, prompting us to search for a suitable starting material for the preparation of the novel [(triphos)$Co^{III}Cl_2$]$^+$ complex **12**$^+$. Its synthesis and characterization including X-ray structural analysis is achieved by the substitution of the catecholato ligand in [(triphos)Co^{III}(cat)]$^+$ complexes[1f,7] by chloride ions in the form of boron trichloride making use of the high affinity of boron to oxygen donor atoms.[8] This reaction is also of particular interest since five-coordinate Co^{III} complexes especially with simple monodentate coligands are relatively rare.[9]

Experimental Section

Materials. 1,1,1-Tris((diphenylphosphino)methyl)ethane, $CH_3C(CH_2PPh_2)_3$,[10] $CoCl_2$,[11] (Catecholato)[1,1,1-tris((diphenylphosphino)methyl)ethane]cobalt(III) tetrafluoroborate,[7] and (4,5-(Methylenedioxy)catecholato)[1,1,1-tris((diphenylphosphino)methyl)ethane]cobalt(III) tetrafluoroborate[1f] were prepared by literature procedures. All other reagents were commercially available. Boron trichloride was stored under inert gas at −70 °C, and a portion (2 mL) was condensed first into a calibrated Schlenk tube cooled to −100 °C and then redistilled into the reaction Schlenk tube. Anhydrous $CoCl_2$ was dissolved in THF to form the adduct $CoCl_2(THF)_x$ by sonicating the initial suspension until a clear, bright blue solution resulted (approximately 20 min).

Bis(μ-chloro)bis[1,1,1-tris((diphenylphosphino)methyl)ethane]dicobalt(II) Bis(tetraphenylborate [1(BPh_4)$_2$]. This compound was prepared either by the procedure of Sacconi et al.[3] in alcohol (ethanol or 1-butanol)/CH_2Cl_2 or in pure THF. To remove the NaCl a solution of the crude complex in CH_2Cl_2 was filtered through 5 cm of Kieselguhr. Recrystallization from THF/Et_2O afforded crystals of the Et_2O solvate suitable for X-ray crystallographic analysis. Recrystallization from CH_2Cl_2/Et_2O yielded the CH_2Cl_2 solvate.[3] Both were obtained in 60−80% yields. Mp: 162−168 °C (dec; both solvates). IR (CsI, CH_2Cl_2 solvate): $\tilde{\nu}$ = 3056 (m), 3034 (m), 2985 (m), 3013 (m), 1640 (br), 1606 (m), 1578 (m), 1482 (s), 1435 (s), 1392 (w), 1332 (w), 1311 (w), 1266 (m), 1181 (w), 1132 (br), 1117 (w), 1096 (s), 1168 (m), 1029 (m), 998 (m), 963 (w), 914 (w), 837 (s), 742 (s), 732 (s), 705 (s), 696 (s), 611 (s), 544 (w), 511 (s), 481 cm^{-1} (m). MS (FAB) [*m/z* (%)]: 717 (70) [triphosCoCl]$^+$, 699 (51) [triphosCo + O]$^+$, 683 (55) [triphosCo]$^+$, 672 (100) [triphos + 3O]$^+$, 656 (42) [triphos + 2O]$^+$, 640 (8) [triphos + O]$^+$, 595 (8) [triphos − Ph + 3O]$^+$, 579 (20) [triphos − Ph + 2O]$^+$, 563 (20) [triphos − Ph + O]$^+$, 547 (18) [triphos − Ph]$^+$. CV (CH_2Cl_2): E_p = −240 mV (irr), E_p (reverse scan) = ±0 mV, E_p = 1125 mV (irr), E_p (reverse scan) = 220 mV. Anal. Calcd for $C_{130}H_{118}P_6Co_2Cl_2B_2$·4$CH_2Cl_2$: C, 66.61; H, 5.26; P, 7.69. Found: C, 66.99; H, 5.37; P, 7.76. Calcd for $C_{130}H_{118}P_6Co_2Cl_2B_2$·1$Et_2O$: C, 74.83; H, 6.00; P, 8.34; Cl, 3.30. Found: C, 73.41; H, 6.19; P, 8.34; Cl, 3.46.

Bis(μ-chloro)bis[1,1,1-tris((diphenylphosphino)methyl)ethane]dicobalt(II) Bis(hexafluorophosphate) [1(PF_6)$_2$]. The preparation was similar to the one described above except for substituting $NaBPh_4$ with $NaPF_6$. Recrystallization from THF/Et_2O afforded crystals of the THF solvate in 55% yield. Mp: 168−180 °C (dec). IR (CsI): $\tilde{\nu}$ = 3062 (m), 1652 (br), 1603 (m), 1589 (w), 1484 (m), 1438 (s), 1403 (w), 1335 (w), 1311 (w), 1279 (w), 1191 (w), 1145 (br), 1121 (s), 1092 (s), 1027 (w), 998 (m), 959 (w), 852 (br, PF), 741 (s), 696 (s), 615 (w), 557 (s), 513 (s), 481 cm^{-1} (w). MS (FAB) [*m/z* (%)]: 717 (100) [triphosCoCl]$^+$, 699 (52) [triphosCo + O]$^+$, 683 (78) [triphosCo]$^+$, 672 (88) [triphos + 3O]$^+$, 656 (50) [triphos + 2O]$^+$, 640 (12) [triphos + O]$^+$, 595 (16) [triphos − Ph + 3O]$^+$, 579 (29) [triphos − Ph + 2O]$^+$, 563 (32) [triphos − Ph + O]$^+$, 547 (28) [triphos − Ph]$^+$. CV (CH_2Cl_2): E_p = −205 mV (irr), E_p (reverse scan) = +25 mV, E_p = 1020 mV (irr), E_p (reverse scan) = 280 mV. Anal. Calcd for $C_{82}H_{78}P_8Co_2Cl_2F_{12}$·3.5THF: C, 58.22; H, 5.39; P, 12.51. Found: C, 58.63; H, 5.15; P, 13.01.

[1,1,1-Tris((diphenylphosphino)methyl)ethane]cobalt(II) Dichloride (3). A solution of the triphos ligand (624 mg, 1 mmol) in THF (20 mL) was added to a solution of anhydrous $CoCl_2$ (130 mg, 1 mmol) in THF (20 mL) resulting in a color change to deep dark blue (compound **2**). Evaporation of the solvent gave a red microcrystalline product. Recrystallization from THF/Et_2O or benzene/Et_2O gave large red needles suitable for X-ray crystallographic analysis. Yield: 60−70%. In one crystallization experiment (THF/Et_2O) additionally to red **3** blue crystals of **1**($CoCl_3THF$)$_2$ were obtained. Mp: 162 °C (dec). IR (CsI): $\tilde{\nu}$ = 3057 (m), 2972 (m), 2926 (m), 1652 (br), 1606 (m), 1483 (s), 1455 (w), 1436 (s), 1401 (w), 1336 (w), 1314 (w), 1219 (sh), 1183 (sh), 1160 (br), 1118 (m), 1095 (s), 1050 (m), 1026 (m), 1001 (m), 959 (w), 921 (w), 879 (w), 834 (m), 741 (s), 697 (s), 668 (m), 616 (w), 567 (m), 549 (m), 513 (s), 487 cm^{-1} (m). MS (FAB) [*m/z* (%)]: 717 (100) [triphosCoCl]$^+$, 699 (26) [triphosCo + O]$^+$, 683 (78) [triphosCo]$^+$, 672 (15) [triphos + 3O]$^+$, 656 (19) [triphos + 2O]$^+$, 640 (10) [triphos + O]$^+$, 595 (7) [triphos − Ph + 3O]$^+$, 579 (15) [triphos − Ph + 2O]$^+$, 563 (15) [triphos − Ph + O]$^+$, 547 (56) [triphos − Ph]$^+$. CV (CH_2Cl_2): E_p = −830 mV (irr), E_p (reverse scan) = +35 mV, $E_{1/2}$ = 335 mV (rev oxidation). Anal. Calcd for $C_{41}H_{39}P_3CoCl_2$: C, 65.27; H, 5.21; P, 12.32; Cl, 9.40. Found: C, 65.22; H, 6.46; P, 11.97; Cl, 9.26.

[1,3-Bis(diphenylphosphino)propane]cobalt(II) Dichloride (4). A solution of the ligand 1,3-bis(diphenylphosphino)propane (412 mg, 1 mmol) in THF (20 mL) was added to a solution of anhydrous $CoCl_2$ (130 mg, 1 mmol) in THF (20 mL) resulting in a color change to deep dark blue. Evaporation of the solvent gave a bright blue microcrystalline product. Recrystallization from CH_2Cl_2/Et_2O gave large blue crystals suitable for X-ray crystallographic analysis. Yield: 78%. Mp: 230 °C. IR (CsI): $\tilde{\nu}$ = 3075 (m), 3054 (m), 2946 (w), 1603 (m), 1485 (s), 1437 (s), 1185 (m), 1160 (m), 1105 (s), 998 (m), 967 (s), 815 (m), 784 (m), 746 (s), 699 (s), 639 (m), 615 (w), 508 (s), 478 (m), 467 cm^{-1} (m). MS (EI) [*m/z* (%)]: 541 (12) [M]$^+$, 506 (4) [M − Cl]$^+$, 429 (4) [M − Cl − Ph]$^+$, 412 (80) [M − $CoCl_2$]$^+$, 335 (100) [M − $CoCl_2$ − Ph]$^+$. Anal. Calcd for $C_{27}H_{26}P_2CoCl_2$: C, 59.80; H, 4.83; P, 11.42; Cl, 13.08. Found: C, 59.75; H, 5.05; P, 11.47; Cl, 12.79.

Bis(μ-chloro)bis[1,1,1-tris((diphenylphosphino)methyl)ethane]dicobalt(II) Hexachlorodizincate [1(Zn_2Cl_6)]. To a THF solution (20 mL) of **2** (1 mmol) was added a solution of $ZnCl_2$·Et_2O in CH_2Cl_2 (2.2 M, 0.5 mL) causing a color change from blue to red. The solution was concentrated in vacuo until **1**(Zn_2Cl_6) started to precipitate. The precipitate was washed with THF and Et_2O, recrystallized from CH_2Cl_2/Et_2O, and dried in vacuo. Yield: 55%. Vapor diffusion of Et_2O into a CH_2Cl_2 solution of the complex afforded red-brown crystals suitable for X-ray crystallographic analysis. Mp: 166−175 °C (dec). IR (CsI): $\tilde{\nu}$ = 3055 (m), 2979 (m), 1603 (m), 1484 (s), 1435 (s), 1188 (m), 1156 (w), 1096 (s), 1065 (m), 998 (m), 914 (w), 882 (w), 832 (m), 744 (s), 698 (s), 513 (s), 481 (m), 474 cm^{-1} (m). MS (FAB) [*m/z* (%)]: 717 (100) [triphosCoCl]$^+$, 699 (7) [triphosCo + O]$^+$, 682 (18) [triphosCo]$^+$, 672 (5) [triphos + 3O]$^+$, 657 (17) [triphos + 2O]$^+$, 640 (6) [triphos + O]$^+$, 578 (6) [triphos − Ph + 2O]$^+$, 563 (13) [triphos −

(6) (a) Connelly, N. G.; Geiger, W. E. *Chem. Rev.* **1996**, *96*, 887. (b) Pevear, K. A.; Banaszak, M. M.; Carpenter, G. B.; Rieger, A. L.; Rieger, P. H.; Sweigard, D. A. *Organometallics* **1995**, *14*, 512. (c) Briggs, T. N.; Jones, C. J.; McCleverty, J. A.; Neaves, B. D.; Murr, N. E.; Colquhoun, H. M. *J. Chem. Soc., Dalton Trans.* **1985**, 1249. (d) Nelsen, S. F.; Hintz, P. J. *J. Am. Chem. Soc.* **1972**, *94*, 7114.

(7) Vogel, S.; Huttner, G.; Zsolnai, L. *Z. Naturforsch.* **1993**, *48b*, 641.

(8) (a) Gerrard, W.; Lappert, M. F.; Mountfield, B. A. *J. Chem. Soc.* **1959**, 1529. (b) Blau, J. A.; Gerrard, W.; Lappert, M. F.; Mountfield, A.; Pyszora, H. *J. Chem. Soc.* **1960**, 380. (c) Wieber, M.; Künzel, W. *Z. Anorg. Allg. Chem.* **1974**, *403*, 107. (d) Bonner, T. G.; Saville, N. M. *J. Chem. Soc.* **1960**, 2851. (e) Teitel, S.; O'Brien, J.; Brossi, A. *J. Org. Chem.* **1972**, *37*, 3368. (e) McOmie, J. F. W.; Watts, M. L.; West, D. E. *Tetrahedron* **1968**, *24*, 2289.

(9) (a) Jensen, K. A.; Nygaard, B.; Pederson, C. T. *Acta Chem. Scand.* **1963**, *17*, 1126. (b) Levason, W.; Ogden, J. S.; Spicer, M. D. *Inorg. Chem.* **1989**, *28*, 2128. (c) Jaynes, B. S.; Ren, T.; Liu, S.; Lippard, S. J. *J. Am. Chem. Soc.* **1992**, *114*, 9670. (d) Brückner, S.; Callgaris, M.; Nardin, G.; Randacio, L. *Inorg. Chim. Acta* **1969**, *3*, 308. (e) Marzilli, L. G.; Summers, M. F.; Bresciani-Pahor, N.; Zangrando, E.; Charland, J.-P.; Randaccio, L. *J. Am. Chem. Soc.* **1985**, *107*, 6880.

(10) Muth, A. Diplomarbeit, University of Heidelberg, 1989.

(11) Heyn, B.; Hipler, B.; Kreisel, G.; Schreer, H.; Walther, D. *Inorganic Synthetic Chemistry*; Springer Verlag: Berlin, Heidelberg, New York, London, Paris, Tokyo, 1986.

Ph + O]$^+$, 547 (22) [triphos − Ph]$^+$. Anal. Calcd for $C_{82}H_{78}P_6Co_2Cl_8Zn_2 \cdot 2CH_2Cl_2$: C, 51.70; H, 4.24; P, 9.52. Found: C, 51.82; H, 4.42; P, 9.60.

{[1,1,1-Tris((diphenylphosphino)methyl)ethane]cobalt(II)}bis(μ-chloro)iron(II) Dichloride (5). To a THF solution (20 mL) of **2** (1 mmol) was added a solution of $FeCl_2$ (127 mg, 1 mmol) in THF (15 mL) causing a color change from blue to red-brown. The solution was concentrated in vacuo until **5** started to precipitate. The precipitate was washed with THF and Et_2O, recrystallized from CH_2Cl_2/Et_2O, and dried in vacuo. Yield: 43%. Vapor diffusion of Et_2O into a CH_2Cl_2 solution of the complex afforded red-brown crystals suitable for X-ray crystallographic analysis. Mp: 205 °C (dec). IR (CsI): $\tilde{\nu}$ = 3056 (m), 2964 (m), 1603 (m), 1485 (s), 1436 (s), 1188 (w), 1160 (w), 1096 (s), 1069 (m), 1027 (m), 998 (m), 878 (w), 829 (m), 815 (w), 745 (s), 697 (s), 515 (s), 485 (m), 474 cm^{-1} (m). MS (FAB) [*m/z* (%)]: 717 (100) [triphosCoCl]$^+$, 699 (8) [triphosCo + O]$^+$, 682 (18) [triphosCo]$^+$, 672 (6) [triphos + 3O]$^+$, 657 (22) [triphos + 2O]$^+$, 640 (40) [triphos + O]$^+$, 578 (8) [triphos − Ph + 2O]$^+$, 563 (54) [triphos − Ph + O]$^+$, 547 (18) [triphos − Ph]$^+$. Anal. Calcd for $C_{41}H_{39}P_3CoCl_4Fe \cdot 1.5CH_2Cl_2$: C, 50.61; H, 4.20. Found: C, 50.94; H, 4.30.

{[1,1,1-Tris((diphenylphosphino)methyl)ethane]cobalt(II)}bis(μ-chloro)cobalt(II) Dichloride (6). To a THF solution (20 mL) of **2** (1 mmol) was added a solution of $CoCl_2$ (130 mg, 1 mmol) in THF (15 mL) causing a color change from blue to violet and the immediate precipitation of **6**. The violet precipitate was washed with THF and Et_2O, recrystallized from CH_2Cl_2/Et_2O, and dried in vacuo. Yield: 86%. Vapor diffusion of Et_2O into a highly dilute CH_2Cl_2 solution of the complex afforded few violet crystals suitable for X-ray crystallographic analysis. Mp: 140 °C (dec). IR (CsI): $\tilde{\nu}$ = 3058 (m), 2980 (m), 1607 (m), 1484 (m), 1437 (s), 1180 (w), 1160 (w), 1093 (s), 1072 (sh), 998 (m), 878 (w), 829 (m), 741 (s), 696 (s), 515 (s), 485 (m), 459 cm^{-1} (w). MS (FAB) [*m/z* (%)]: 717 (100) [triphosCoCl]$^+$, 699 (16) [triphosCo + O]$^+$, 682 (32) [triphosCo]$^+$, 672 (11) [triphos + 3O]$^+$, 657 (16) [triphos + 2O]$^+$, 640 (5) [triphos + O]$^+$, 578 (5) [triphos − Ph + 2O]$^+$, 563 (16) [triphos − Ph + O]$^+$, 547 (48) [triphos − Ph]$^+$. Anal. Calcd for $C_{41}H_{39}P_3Co_2Cl_4 \cdot 0.5CH_2Cl_2$: C, 53.78; H, 4.35; P, 10.03. Found: C, 53.80; H, 5.02; P, 9.28.

[1,1,1-Tris((diphenylphosphino)methyl)ethane](trimethylphosphine)cobalt(II) Chloride Tetraphenylborate [8(BPh$_4$)]. To a THF solution (20 mL) of **2** (1 mmol) was added a solution of PMe_3 in THF (1 M, 1 mL) causing a slow color change from blue to green. The reaction was accelerated by the addition of solid $NaBPh_4$ (342 mg, 1 mmol). After removal of solvent the green solid residue was taken up in CH_2Cl_2 and filtered through 5 cm of Kieselguhr. Recrystallization from CH_2Cl_2/Et_2O afforded **8**(BPh_4) in 86% yield. Vapor diffusion of Et_2O into a CH_2Cl_2 solution of the complex afforded large dichroic (red/green) crystals suitable for X-ray crystallographic analysis. Mp: 165 °C. IR (CsI): $\tilde{\nu}$ = 3056 (m), 2999 (m), 2981 (m), 2918 (m), 2868 (m), 1603 (m), 1578 (m), 1480 (s), 1436 (s), 1279 (m), 1160 (sh), 1142 (sh), 1118 (sh), 1093 (s), 1029 (m), 998 (m), 948 (s, P-CH_3), 843 (m), 741 (s), 730 (s), 703 (s), 692 (s), 611 (m), 514 (s), 478 (m), 446 cm^{-1} (m). MS (FAB) [*m/z* (%)]: 794 (4) [M]$^+$, 717 (100) [triphosCoCl]$^+$, 682 (10) [triphosCo]$^+$, 640 (3) [triphos + O]$^+$, 547 (14) [triphos − Ph]$^+$. CV (CH_2Cl_2): E_p = −835 mV (irr), E_p (reverse scan) = 35 mV, E_p = 920 mV (irr). Anal. Calcd for $C_{68}H_{68}P_4CoClB \cdot 1CH_2Cl_2$: C, 69.10; H, 5.88; P, 10.33; Cl, 8.87. Found: C, 69.13; H, 6.13; P, 10.23; Cl, 8.66.

[1,1,1-Tris((diphenylphosphino)methyl)ethane](ammine)cobalt(II) Chloride Tetraphenylborate [9(BPh$_4$)]. To a THF solution (20 mL) of **2** (1 mmol) was added 5 mL of a THF solution saturated with gaseous ammonia (direct bubbling of ammonia into the THF solution of **3** leads to decomposition). No color change was observed. The reaction was initiated by the addition of solid $NaBPh_4$ (342 mg, 1 mmol) resulting in a color change from blue to orange-brown. After removal of solvent the brown solid residue was taken up in CH_2Cl_2 and filtered through 5 cm of Kieselguhr. Yield: 85%. Vapor diffusion of Et_2O/THF mixtures saturated with NH_3 into a CH_2Cl_2 solution of the complex afforded small orange needles suitable for X-ray crystallographic analysis. Recrystallization from CH_2Cl_2/Et_2O or THF/Et_2O yielded only crystals of the corresponding solvates of **1**(BPh_4)$_2$. Mp: 155 °C (dec). IR (CsI): $\tilde{\nu}$ = 3359 (w), 3347 (w), 3321 (w), 3248 (m), 3197 (w) (N−H), 3056 (m), 2999 (m), 2981 (m), 2918 (m), 1606 (m), 1582 (m), 1480 (s), 1435 (s), 1262 (s), 1160 (sh), 1146 (m), 1118 (m), 1093 (s), 1029 (m), 998 (m), 839 (m), 740 (sh), 733 (s), 702 (s), 693 (sh), 611 (m), 515 (s), 481 (m). IR (CH_2Cl_2): $\tilde{\nu}$ = 3356, 3346, 3336, 3263, 3215 cm^{-1} (m, N−H). MS (FAB) [*m/z* (%)]: 717 (100) [triphosCoCl]$^+$, 699 (11) [triphosCo + O]$^+$, 683 (34) [triphosCo]$^+$, 672 (5) [triphos + 3O]$^+$, 656 (20) [triphos + 2O]$^+$, 640 (4) [triphos + O]$^+$, 579 (9) [triphos − Ph + 2O]$^+$, 563 (5) [triphos − Ph + O]$^+$, 547 (13) [triphos − Ph]$^+$. CV (CH_2Cl_2): E_p = −720 mV (irr), E_p (reverse scan) = 35 mV, E_p = 880 mV (irr), E_p (reverse scan) = 260 mV. Anal. Calcd for $C_{65}H_{62}NP_3CoClB$: C, 73.98; H, 5.92; N, 1.33; P, 8.80; Cl, 3.36. Found: C, 72.73; H, 6.27; N, 1.07; P, 8.76; Cl, 3.69.

[1,1,1-Tris((diphenylphosphino)methyl)ethane](acetonitrile)cobalt(II) Chloride Tetraphenylborate [10(BPh$_4$)]. To a THF solution (20 mL) of **2** (1 mmol) was added 5 mL of acetonitrile. No color change was observed. The reaction was initiated by the addition of solid $NaBPh_4$ (342 mg, 1 mmol) resulting in a color change from blue to orange-brown. After removal of solvent the brown solid residue was taken up in CH_2Cl_2, filtered through 5 cm of Kieselguhr, and dried. Yield: 70% (of the CH_2Cl_2 solvate). Vapor diffusion of Et_2O into a CH_3CN solution of the complex afforded orange crystals of the CH_3CN solvate suitable for X-ray crystallographic analysis. Recrystallization from CH_2Cl_2/Et_2O yielded only crystals of the CH_2Cl_2 solvate of **1**(BPh_4)$_2$. Mp: 160−167 °C (dec). IR (CsI): $\tilde{\nu}$ = 3056 (m), 2984 (m), 2290 (w, CN), 1603 (w), 1578 (m), 1484 (s), 1436 (s), 1185 (m), 1137 (m), 1121 (m), 1093 (s), 1068 (m), 1029 (m), 998 (m), 843 (m), 745 (sh), 735 (s), 705 (s), 697 (sh), 611 (m), 513 (s), 481 (m), 450 cm^{-1} (w). MS (FAB) [*m/z* (%)]: 717 (100) [triphosCoCl]$^+$, 699 (32) [triphosCo + O]$^+$, 683 (58) [triphosCo]$^+$, 672 (88) [triphos + 3O]$^+$, 656 (48) [triphos + 2O]$^+$, 640 (6) [triphos + O]$^+$, 624 (10) [triphos]$^+$, 595 (8) [triphos − Ph + 3O]$^+$, 579 (18) [triphos − Ph + 2O]$^+$, 563 (14) [triphos − Ph + O]$^+$, 547 (20) [triphos − Ph]$^+$. CV (CH_2Cl_2): E_p = −180 mV (irr), E_p (reverse scan) = 20 mV, E_p = 880 mV (irr), E_p (reverse scan) = 320 mV. Anal. Calcd for $C_{67}H_{62}NP_3CoClB \cdot 1CH_2Cl_2$: C, 70.15; H, 5.54; N, 1.20; P, 7.98. Found: C, 70.63; H, 5.54; N, 0.82; P, 8.08 (the low N value measured might be due to loss of CH_3CN).

[1,1,1-Tris((diphenylphosphino)methyl)ethane]cobalt(I) Chloride (11). To a THF solution (20 mL) of **2** (1 mmol) was added a solution of $BH_3 \cdot$THF in THF (1 M, 3 mL) resulting in a color change from blue to green. After 10 mL of EtOH was added and the solution was stirred for 15 min yellow **11** started to precipitate. The microcrystalline, highly air-sensitive powder was separated by filtration, washed with EtOH and Et_2O, and dried in vacuo. Yield: 33%. Orange crystals suitable for X-ray crystallographic analysis were obtained by vapor diffusion of Et_2O into a THF solution of the complex. Mp: 160−170 °C (dec). IR (CsI): $\tilde{\nu}$ = 3052 (m), 2953 (m), 1603 (m), 1585 (m), 1480 (m), 1452 (w), 1436 (s), 1185 (m), 1153 (w), 1117 (sh), 1094 (s), 1072 (w), 1023 (m), 998 (m), 833 (m), 746 (sh), 736 (s), 706 (sh), 696 (s), 615 (w), 514 (s), 478 (m), 463 cm^{-1} (w). MS (FAB) [*m/z* (%)]: 749 (5) [triphosCoCl + 2O]$^+$, 733 (20) [triphosCoCl + O]$^+$, 717 (5) [triphosCoCl]$^+$, 699 (18) [triphosCo + O]$^+$, 683 (28) [triphosCo]$^+$, 672 (80) [triphos + 3O]$^+$, 656 (100) [triphos + 2O]$^+$, 640 (8) [triphos + O]$^+$, 595 (8) [triphos − Ph + 3O]$^+$, 579 (30) [triphos − Ph + 2O]$^+$, 563 (27) [triphos − Ph + O]$^+$, 547 (4) [triphos − Ph]$^+$. CV (CH_2Cl_2): E_p = 67 mV (irr), E_p (reverse scan) = −175 mV, $E_{1/2}$ = 760 mV (qrev), $E_{1/2}$ = 980 mV (qrev). Anal. Calcd for $C_{41}H_{39}P_3CoCl$: C, 68.48; H, 5.47. Found: C, 67.78; H, 5.56.

[1,1,1-Tris((diphenylphosphino)methyl)ethane]cobalt(III) Dichloride Tetrachloroborate [12(BCl$_4$)]. A solution of (4,5-methylenedioxy-catecholato)[1,1,1-tris((diphenylphosphino)methyl)ethane]cobalt(III) tetrafluoroborate (922 mg, 1 mmol) or (catecholato)[1,1,1-tris((diphenylphosphino)methyl)ethane]cobalt(III) tetrafluoroborate (878 mg, 1 mmol) in CH_2Cl_2 (20 mL) was added dropwise to a freshly prepared solution of 2 mL of BCl_3 in CH_2Cl_2 (10 mL) at −60 °C. The color immediately changed from blue to brown-green. After the mixture was stirred for 15 min at −60 °C it was allowed to warm to room temperature. Excess BCl_3 was removed in vacuo, and the solution was concentrated to 15 mL. Overlayering the solution with Et_2O yielded dark green cubic shaped crystals of **12**(BCl_4). Yield: 15−20%. Mp: 200 °C (dec). IR (CsI): $\tilde{\nu}$ = 3064 (m), 1607 (w), ≈1500 (br), 1484 (m), 1436 (s), 1194 (m), 1165 (m), 1089 (m), 1048 (w), 1000 (m), 882 (m), 857 (m), 740 (s), 689 (s), 540 (m), 510 (s), 484 (m), 458 cm^{-1} (w). MS (FAB) [*m/z* (%)]: 717 (100) [triphosCoCl]$^+$, 683 (22) [triphosCo]$^+$, 672 (19) [triphos + 3O]$^+$, 656 (45) [triphos + 2O]$^+$,

Table 1. Crystallographic Data for **1**$(BPh_4)_2$, **3**, **1**(Zn_2Cl_6), **1**$(CoCl_3THF)_2$, **4**, and **5**

	1$(BPh_4)_2$·Et_2O	**3**·0.2Et_2O	**1**(Zn_2Cl_6)·CH_2Cl_2	**1**$(CoCl_3THF)_2$·1.5THF	**4**	**5**·0.8CH_2Cl_2
formula (without solvates)	$C_{130}H_{118}P_6Co_2Cl_2B_2$	$C_{41}H_{39}P_3CoCl_2$	$C_{82}H_{78}P_6Co_2Cl_8Zn_2$	$C_{90}H_{94}P_6Co_4Cl_8O_2$	$C_{27}H_{26}P_2CoCl_2$	$C_{41}H_{39}P_3CoFeCl_4$
M_r (without solvates)	2076.6	754.5	1781.6	1912.9	542.3	881.3
cryst size/mm	0.30 × 0.30 × 0.30	0.10 × 0.10 × 0.40	0.30 × 0.20 × 0.20	0.40 × 0.40 × 0.30	0.50 × 0.40 × 0.30	0.30 × 0.30 × 0.30
cryst system	monoclinic	hexagonal	triclinic	triclinic	monoclinic	monoclinic
Z	4	6	1	1	4	4
space group (No.)	$C2/c$ (15)	$P6_1$ (169)	$P\bar{1}$ (2)	$P\bar{1}$ (2)	$P2_1/c$ (14)	$P2_1/n$ (14)
a/Å	23.808(3)	20.015(4)	12.782(1)	13.059(1)	15.075(2)	12.808(1)
b/Å	16.544(4)	20.015(4)	12.819(1)	13.796(1)	11.129(3)	19.632(2)
c/Å	30.260(4)	16.516(5)	13.943(1)	14.526(1)	15.249(2)	17.038(2)
α/deg	90.00(0)	90.00(0)	79.76(1)	105.18(1)	90.00(0)	90.00(0)
β/deg	76.94(1)	90.00(0)	71.41(1)	98.34(1)	89.39(1)	92.13(1)
γ/deg	90.00(0)	120.00(0)	81.90(1)	105.93(1)	90.00(0)	90.00(0)
V/Å^3	11 611(4)	5730(2)	2122.2(3)	2361.4(3)	2558.2(8)	4281.2(7)
ρ(calcd)/g cm^{-3}	1.225	1.334	1.527	1.407	1.408	1.470
T/K	200	200	200	200	200	200
2θ range/deg	3.0−50.0	3.4−49.0	4.2−50.0	4.7−54.0	4.5−50.4	4.1−48.0
scan speed/deg min^{-1}	$\dot{\omega} = 10.0$	$\dot{\omega} = 8.0$	$\dot{\omega} = 12.0$	$\dot{\omega} = 11.0$	$\dot{\omega} = 14.0$	$\dot{\omega} = 12.0$
no. rflns measd	10 488	9217	7826	10 621	4685	7039
no. unique rlfns	10 224	3906	7463	10 161	4502	6710
no. reflns obsd	6894	2646	5661	8128	3682	4332
obsd criterion	$I > 2\sigma(I)$	$I > 2\sigma(I)$	$I > 2\sigma(I)$	$I > 2\sigma(I)$	$I > 2\sigma(I)$	$I > 2\sigma(I)$
no. of params	678	371	507	749	291	524
R_1/%[a]	6.5	7.6	4.1	4.7	5.2	6.6
R_w/% (refinement on F^2)[b]	20.2	18.9	9.1	13.9	13.8	16.7

[a] $R_1 = \sum||F_o| - |F_c||/\sum|F_o|$. [b] $R_w = [\sum w(F_o^2 - F_c^2)^2/\sum w(F_o^2)^2]^{0.5}$, where w = weighting factor.

640 (30) [triphos + O]$^+$, 624 (21) [triphos]$^+$, 579 (11) [triphos − Ph + 2O]$^+$, 563 (28) [triphos − Ph + O]$^+$, 547 (88) [triphos − Ph]$^+$. CV (CH_2Cl_2): $E_{1/2}$ = 340 mV (rev. Red.), E_p = −1150 mV (irr), E_p (reverse scan) = 0 mV. ^{1}H-NMR (CD_2Cl_2): 2.13 (bs, 3 H, CH_3), 2.66 (bs, 6 H, CH_2), 7.1−7.5 (m, 30 H, CH_{ar}). ^{31}P-NMR (CD_2Cl_2): 26.6 (s). ^{13}C-NMR (CD_2Cl_2): 32.3 (m, *C*H$_3$), 36.6 (m, *C*H$_2$), 40.3 (s, C$_q$), 129.4, 132.5, 133.8, 138.3 (s, C_{ar}). ^{11}B-NMR (CD_2Cl_2): 7.0 (s, *B*Cl$_4$). Anal. Calcd for $C_{41}H_{39}P_3CoCl_6B$·0.5CH_2Cl_2: C, 52.49; H, 4.25. Found: C, 52.28; H, 4.51.

[1,1,1-Tris((diphenylphosphino)methyl)ethane]cobalt(III) Dichloride Tetrafluoroborate [12(BF$_4$)]. A solution of (Cp_2Fe)(BF_4) (248 mg, 0.9 mmol) in CH_2Cl_2 (20 mL) was added at once to a solution of **3** (1 mmol) in CH_2Cl_2 (20 mL). The color changed from red to green. Additional (Cp_2Fe)(BF_4) dissolved in CH_2Cl_2 was added until the UV/vis spectrum showed the absence of unreacted **3**. The solvent was evaporated and the solid green residue extracted with Et_2O (20 mL) until the Et_2O was colorless (6−8×). The green powder was dissolved in a small amount of CH_2Cl_2, precipitated by addition of Et_2O (3×), and finally dried in vacuo. Yield: 92%. Mp: 215 °C (dec). IR (CsI): $\tilde{\nu}$ = 3062 (m), 1606 (w), 1584 (w), 1573 (w), 1483 (m), 1434 (s), 1193 (m), 1162 (m), 1088 (s), 1059 (br), 999 (m), 834 (m), 740 (s), 692 (s), 510 (s), 475 cm^{-1} (m). MS (FAB) [*m*/*z* (%)]: 753 (19) [M]$^+$, 734 (15) [triphosCoCl + O]$^+$ 717 (100) [triphosCoCl]$^+$, 683 (8) [triphosCo]$^+$, 672 (8) [triphos + 3O]$^+$, 656 (19) [triphos + 2O]$^+$, 640 (12) [triphos + O]$^+$, 579 (6) [triphos − Ph + 2O]$^+$, 563 (12) [triphos − Ph + O]$^+$, 547 (33) [triphos − Ph]$^+$. CV (CH_2Cl_2): $E_{1/2}$ = 340 mV (rev reduction). ^{1}H-NMR (CD_2Cl_2): 2.10 (bs, 3 H, CH_3), 2.65 (bs, 6 H, CH_2), 7.1−7.5 (m, 30 H, CH_{ar}). ^{31}P-NMR (CD_2Cl_2): 27.0 (s). ^{13}C-NMR (CD_2Cl_2): 32.1 (m, *C*H$_3$), 35.6 (m, *C*H$_2$), 40.0 (s, C$_q$), 130−138 (C_{ar}). ^{11}B-NMR (CD_2Cl_2): −0.1 (s, *B*F$_4$). Anal. Calcd for $C_{41}H_{39}P_3CoCl_2BF_4$·0.5$CH_2Cl_2$: C, 56.40; H, 4.56; P, 10.51. Found: C, 56.83; H, 5.00; P, 10.26.

Physical Measurements. All manipulations were carried out under an inert atmosphere by means of standard Schlenk techniques. All solvents were dried by standard methods and distilled under inert gas. NMR: Bruker AC 200 at 200.13 MHz (^{1}H), 50.323 MHz (^{13}C{^{1}H}), 81.015 MHz (^{31}P{^{1}H}), 64.210 MHz (^{11}B{^{1}H}); chemical shifts (δ) in ppm with respect to CD_2Cl_2 (^{1}H, δ = 5.32; ^{13}C, δ = 53.5) as internal standard, to H_3PO_4 (^{31}P, δ = 0), and to BF_3·OEt_2 (^{11}B, δ = 0) as external standards. IR: Bruker FTIR IFS-66, as CsI disks. UV/vis/NIR: Perkin-Elmer Lambda 19, Oxford temperature control unit ITC-4, Oxford cryostat DN-1704. MS (FAB): Finnigan MAT 8230, 4-nitrobenzyl alcohol matrix. EPR: Bruker ESP 300 E, X-band, standard cavity ER 4102, temperature control unit Eurotherm B-VT 2000, external standard diphenylpicrylhydrazyl (DPPH). Elemental analyses: microanalytical laboratory of the Organisch-Chemisches Institut, University of Heidelberg. Melting points: Gallenkamp MFB-595 010, melting points are not corrected. Cyclic voltammetry: Metrohm "Universal Mess- und Titriergefäss", Metrohm GC electrode RDE 628, platinum electrode, SCE electrode, Princeton Applied Research potentiostat Model 273, 10^{-3} M in 0.1 M *n*Bu_4NPF_6/CH_2Cl_2. Magnetic measurements: (a) Faraday balance, Bruker electromagnet B-E 15 C8, Bruker field controler B-H 15, Sartorius vacuum-microbalance M 25 D-S, Oxford temperature control unit ITC-4, Oxford He-evaporator cryostat CF 1200, calibration with $K_3[Fe(CN)_6]$; (b) Evans method, calibration with diphenylpicrylhydrazyl (DPPH).[12] Molecular weight determinations: Knauer vapor-pressure osmometer No. 7311100000, calibration with benzil. Conductance measurements: Schott conductivity bridge CG 855 in ca. 10^{-3} M solutions.

Crystallographic Structure Determinations. The measurements were carried out on a Siemens P4 (Nicolet Syntex) R3m/v four-circle diffractometer with graphite-monochromated Mo *K*α radiation. All calculations were performed using the SHELXT PLUS software package. Structures were solved by direct methods with the SHELXS-86 program and refined with the SHELX93 program.[13] An absorption correction (ψ scan, $\Delta\psi$ = 10°) was applied to all data. Atomic coordinates and anisotropic thermal parameters of the non-hydrogen atoms were refined by full-matrix least-squares calculation. Tables 1 and 2 compile the data for the structure determinations. Tables containing a full listing of atom positions, anisotropic displacement parameters, and hydrogen atom locations are available as Supporting Information.

Results And Discussion

Cobalt(II) chloride reacts with triphos and $NaBPh_4$ in alcohol/methylene chloride or alcohol/THF (Scheme 1, left pathway) under inert gas to give red-brown crystals with the empirical formula [(triphos)CoCl](BPh_4)·*x* (solvent).[3] This compound was assigned a dinuclear structure with two bridging chloride ions on the basis of reflectance spectra and magnetic behavior.[3] The assignment of a doubly bridged structure is now confirmed by an X-ray structure determination of the Et_2O solvate of **1**$(BPh_4)_2$ (Figure 1). The presence of these dinuclear species also in solution is corroborated by the high conductivity of those solutions and the similarity of the solution- and solid-state electronic spectra (Tables 3 and 4).

(12) (a) Evans, D. F. *J. Chem. Soc.* **1959**, 2003. (b) Crawford, T. H.; Swanson, J. *J. Chem. Educ.* **1971**, *48*, 382.

(13) (a) Sheldrick, G. M. SHELXS 86, Program for Crystal Structure Solution, University of Göttingen, 1986. (b) Sheldrick, G. M. SHELXL 93, Program for Crystal Structure Refinement, University of Göttingen, 1993.

Table 2. Crystallographic Data for **6**, **8**(BPh_4), **9**(BPh_4), **10**(BPh_4), **11**, and **12**(BCl_4)

	6·CH_2Cl_2	**8**(BPh_4)·CH_2Cl_2	**9**(BPh_4)·CH_2Cl_2	**10**(BPh_4)·2 CH_3CN	**11**	**12**(BCl_4)·$^1/_4CH_2Cl_2$
formula (without solvates)	$C_{41}H_{39}P_3Co_2Cl_4$	$C_{68}H_{68}P_4CoClB$	$C_{65}H_{62}P_3CoClNB$	$C_{67}H_{62}P_3CoClNB$	$C_{41}H_{39}P_3CoCl$	$C_{41}H_{39}P_3CoCl_6B$
M_r (without solvates)	884.4	1114.4	1055.3	1079.4	719.1	907.1
cryst size/mm	0.40 × 0.30 × 0.30	0.40 × 0.40 × 0.40	0.20 × 0.10 × 0.10	0.50 × 0.40 × 0.30	0.20 × 0.30 × 0.30	0.40 × 0.40 × 0.40
cryst system	monoclinic	monoclinic	triclinic	triclinic	orthorhombic	orthorhombic
Z	4	4	2	2	4	16
space group (No.)	$P2_1/n$ (14)	$P2_1/c$ (14)	$P\bar{1}$ (2)	$P\bar{1}$ (2)	$Pna2_1$ (33)	$Iba2$ (45)
a/Å	12.768(2)	10.158(5)	9.661(1)	12.308(3)	20.723(6)	23.452(4)
b/Å	19.657(2)	18.16(1)	15.635(2)	16.249(5)	10.274(4)	23.483(4)
c/Å	16.983(2)	33.22(2)	19.562(2)	17.302(4)	16.871(4)	33.697(7)
α/deg	90.00(0)	90.00(0)	85.94(1)	65.57(2)	90.00(0)	90.00(0)
β/deg	92.11(1)	82.87(4)	83.11(1)	72.27(2)	90.00(0)	90.00(0)
γ/deg	90.00(0)	90.00(0)	73.61(1)	81.95(2)	90.00(0)	90.00(0)
V/Å^3	4259.5(9)	6081(6)	2812.2(5)	3000(1)	3592(2)	18 558(6)
ρ(calcd)/g cm^{-3}	1.508	1.308	1.347	1.285	1.330	1.340
T/K	200	200	200	200	200	200
2θ range/deg	4.1−48.0	4.3−51.0	4.2−50.0	4.0−52.0	3.9−47.0	4.1−51.8
scan speed/deg min^{-1}	$\dot{\omega} = 13.0$	$\dot{\omega} = 14.0$	$\dot{\omega} = 9.0$	$\dot{\omega} = 11.0$	$8.0 < \dot{\omega} < 60.0$	$\dot{\omega} = 10.0$
no. rflns measd	7017	11 729	10 559	12 055	2756	30 309
no. unique rlfns	6687	11 143	9917	11 490	2756	14 611
no. reflns obsd	4888	7970	6129	9317	2290	14 157
obsd criterion	$I > 2\sigma(I)$	$I > 2\sigma(I)$	$I > 2\sigma(I)$	$I > 2\sigma(I)$	$I > 2\sigma(I)$	$I > 2\sigma(I)$
no. of params	492	717	694	893	347	989
R_1/%[a]	5.1	5.5	6.0	4.1	4.8	6.5
R_w/% (refinement on F^2)[b]	13.8	14.5	12.8	10.8	13.7	20.0

[a] $R_1 = \sum||F_o| - |F_c||/\sum|F_o|$. [b] $R_w = [\sum w(F_o^2 - F_c^2)^2/\sum w(F_o^2)^2]^{0.5}$, where w = weighting factor.

Scheme 1. Reaction of triphos with $CoCl_2$

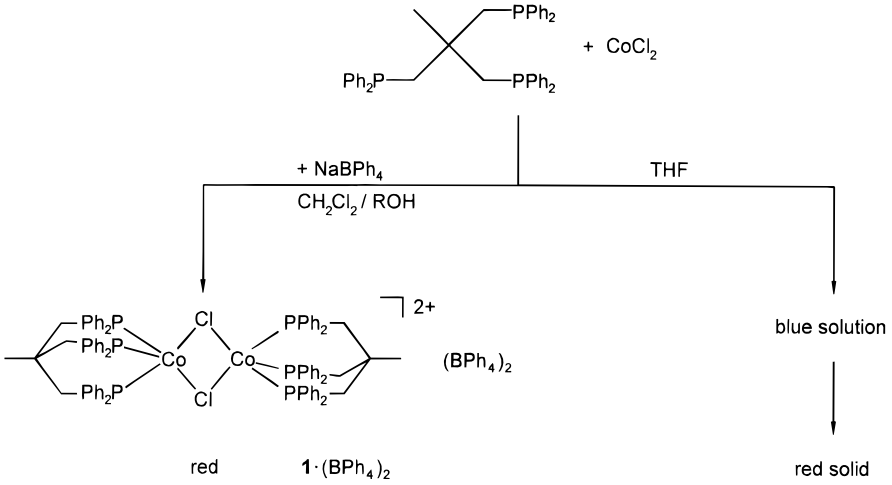

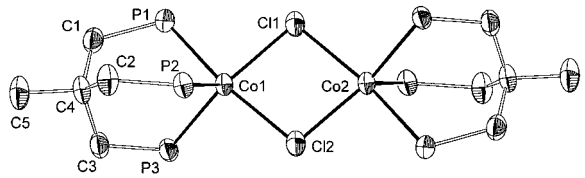

Figure 1. ZORTEP view of the cation of **1**(BPh_4)$_2$.[45]

In the absence of $NaBPh_4$ the reaction of $CoCl_2$ with triphos in THF initially yields a dark *blue* solution which on evaporation of the solvent gives a *red* microcrystalline material of the empirical formula [(triphos)$CoCl_2$] (Scheme 1, right pathway). Redissolving the red compound in THF again forms a blue solution; using methylene chloride instead of THF gives a red solution which on adding THF turns blue. The procedure of dissolving and evaporating can be performed several times, always restoring the blue or red color, respectively. As both solutions (the blue THF and the red CH_2Cl_2 solution) are nonconducting the possibility of ionic species in either of these can be ruled out. The electronic (ligand-field transition around 1000 nm) and the EPR spectra of the red species are very similar to those of the dinuclear $\mathbf{1}^{2+}$ cation; therefore a similar ligand field (3 × P, 2 × Cl) must be present in the red species. This geometric arrangement was confirmed by an X-ray structure determination (Figure 2). The red compound **3** is indeed a mononuclear five-coordinate cobalt complex with a 3 P/2 Cl donor set. The magnetic behavior, EPR, and UV/vis data are consistent with the formulation of a low-spin Co^{II} complex (Tables 3 and 4).[14]

As all attempts to isolate the blue species **2** as a solid were unsuccessful, the properties of **2** were studied in solution. The solution magnetic moment at 295 K studied by the method of Evans[12] is 4.0 μ_B per cobalt, corresponding to three unpaired electrons per cobalt ion. A spectrophotometric titration of triphos with $CoCl_2$ in THF gives a sharp end point corresponding to a 1:1 triphos/$CoCl_2$ ratio identical to that of **3**. Dilution studies in THF (1.56−12.5 mM) show no deviation from Beer's law thereby excluding the formation of dimers or oligomers. Also the molecular mass determined osmometrically in THF corresponds to a mononuclear species (found, 740 ± 80 g mol^{-1},

(14) (a) Sacconi, L.; Mani, F. *Transition Met. Chem.* (N.Y.) **1982**, *8*, 179. (b) Sernau, V.; Huttner, G.; Fritz, M.; Janssen, B.; Büchner, M.; Emmerich, C.; Walter, O.; Zsolnai, L.; Günauer, D.; Seitz, T. *Z. Naturforsch.* **1995**, *50b*, 1638. (c) Heinze, K.; Mann, S.; Huttner, G.; Zsolnai, L. *Chem. Ber.* **1996**, *129*, 1115. (d) Körner, V.; Asam, A.; Huttner, G.; Zsolnai, L.; Büchner, M. *Z. Naturforsch.* **1994**, *49b*, 1183. (e) Asam, A.; Janssen, B.; Huttner, G.; Zsolnai, L.; Walter, O. *Z. Naturforsch.* **1993**, *48b*, 1707. (f) Vogel, S.; Huttner, G.; Zsolnai, L.; Emmerich, C. *Z. Naturforsch.* **1993**, *48b*, 353.

Table 3. Conductivity, Magnetic, and EPR Data

compd	Λ_M (S cm^2 mol^{-1})	μ_{eff} (μ_B), 295 K	EPR, 295 K[e]	EPR, 100 K[e,f]
1$(BPh_4)_2$	47[a]	2.3[b,d] 2.4[c,d,3]	2.13 (23), 2.11 (34)[a]	2.11 (63, 52)[b]
1$(PF_6)_2$	51[a]	2.3[b,d]	2.13 (23), 2.11 (34)[a]	2.11 (63, 52)[b]
2	<1[b]	4.0[b]		
3	<1[a]	2.3[a] 2.1[c]	2.13 (23), 2.11 (34)[a]	2.11 (63, 52)[b]
4	<1[b]	4.2[a]		
1(Zn_2Cl_6)	5[a]	2.5[c,d]	2.13 (23), 2.11 (34)[a]	2.11 (63, 52)[b]
5	12[a]	5.8[c,d]	weak, broad feature[a]	weak, broad feature[b]
6	insoluble	5.0[c,d]	insoluble	insoluble
8(BPh_4)	28[a]	2.0[a]	2.13 (23), 2.10 (29)[a]	2.07 (29, 20)[b]
9(BPh_4)	35[a]	2.1[a]	2.12 (23), 2.10 (29)[a]	2.09 (30, 23)[b]
10(BPh_4)	34[a]	2.0[a]	2.13 (23), 2.10 (29)[a]	2.08 (30, 35)[b]
11	<1[a]	3.0[a]		
12(BF_4)	29[a]			

[a] CH_2Cl_2. [b] THF. [c] Solid. [d] Moment per dinuclear unit. [e] *g*-values; resolved A_{Co} (G) in parentheses. [f] Average *g*-values.

Table 4. Absorption Maxima and Extinction Coefficients

compd	λ_{max} (nm) (ϵ (L mol^{-1} cm^{-1}))
1$(BPh_4)_2$	506 (2115), 1018 (815)[a] 500, 649, (sh), 1000[d,3]
1$(PF_6)_2$	505 (1875), 1011 (785)[a]
2	591 (590), 640 (370), 738 (470), 1156 (125, br), 1387 (110, br)[b] 590 (520), 639 (320), 740 (425), 1092 (130, br), 1409 (100, br)[c]
3	482 (430), 584 (395), 642 (200, sh), 729 (215), 948 (260)[a] 475 (848), 553 (675), 945 (685)[b,e]
4	591 (775), 636 (510), 728 (590), 1197 (125, br), 1395 (140, br)[a] 584 (510), 635 (360), 735 (360), 866 (25), 1195 (80), 1390 (100)[b]
1(Zn_2Cl_6)	494 (920), 582 (780, sh), 642 (330, sh), 685 (300, sh), 728 (400), 979 (620)[a]
5	493 (1190), 578 (790, sh), 641 (450), 725 (390), 984 (570)[a]
6	500 (1180), 566 (780, sh), 682 (750), 729 (780), 1000 (690)[a]
7(BPh_4)	649 (969), 1183 (200)[e,1g]
8(BPh_4)	433 (1050), 734 (652), 1306 (80, br)[a] 433 (890), 736 (620), 1305 (70, br)[b]
9(BPh_4)	449 (720), 500 (430, sh), 787 (500), 1185 (115, br)[a]
10(BPh_4)	450 (470), 564 (190, sh), 808 (350), 1175 (90)[a]
11	530 (120, sh), 826 (150), 1131 (430), 1224 (450)[a]
12(BCl_4)	436 (3100, sh), 637 (740), 664 (650, sh), 695 (470, sh)[a] 625[d]
12(BF_4)	451 (2280, sh), 625 (767 br)[a]

[a] CH_2Cl_2. [b] THF. [c] Benzene. [d] Solid. [e] 178 K. [e] 1,2-Dichloroethane.

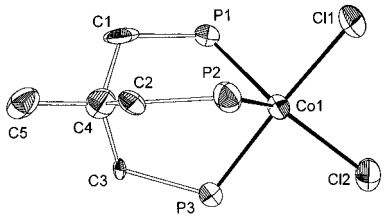

Figure 2. ZORTEP view of **3**.[45]

calcd for [(triphos)$CoCl_2$], 754 g mol^{-1}). Adding chloride ions in the form of $(Ph_4P)Cl$ (100-fold excess) does not change the UV/vis spectrum so the dissociation of chloride was also ruled out. In the 500−700 nm region the electronic spectrum exhibits the characteristic multicomponent band associated with the $^4A_2 \rightarrow {}^4T_1$ transition in tetrahedral or pseudotetrahedral Co^{II} complexes.[15] This prompted us to compare the electronic spectrum of the blue solution with the spectrum of the known pseudotetrahedral (dppp)$CoCl_2$ complex **4** [dppp = 1,3-bis-((diphenylphosphino))propane, $(PPh_2)(CH_2)_3(PPh_2)$] (Table 4).[16]

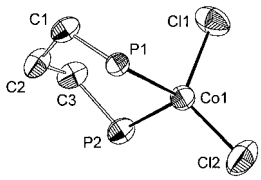

Figure 3. ZORTEP view of **4**.[45]

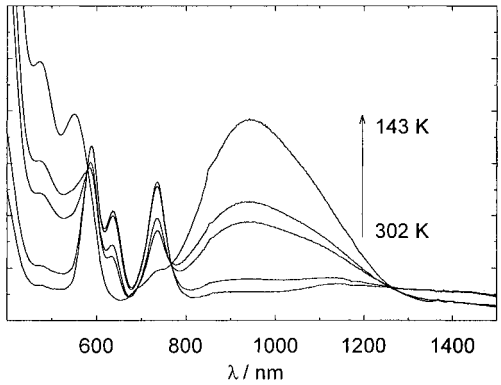

Figure 4. Changes in the optical spectrum of a THF solution of **2** upon cooling.

The four-coordination in **4** is unambigously confirmed by an X-ray structural analysis (Figure 3). Its electronic spectrum is almost superimposable with that of the blue species **2** (Table 4). Similar spectra were observed with multidentate phosphine ligands and $CoCl_2$; these were also interpreted in terms of a 2 P/2 Cl donor set around Co^{II}.[17] This observation together with the above mentioned facts leaves only one interpretation: The blue species **2** is a four-coordinate, mononuclear, nonionic, high-spin [(triphos)$Co^{II}Cl_2$] complex with one dangling phosphorus donor arm (Scheme 2). The triphos ligand acting as a bidentate ligand has been observed previously in [(η^2-triphos)Ni^{II}][18] and [(η^2-triphos)Re^{I}] complexes.[19] Phosphane arm-off reactions have been observed to occur in octahedral [(triphos)Rh^{III}]

(15) (a) Cotton, F. A.; Goodgame, M. *J. Am. Chem. Soc.* **1961**, *83*, 1777. (b) Cotton, F. A.; Goodgame, D. M. L.; Goodgame, M.; Sacco, A. *J. Am. Chem. Soc.* **1961**, *83*, 4157. (c) Cotton, F. A.; Faut, O. D.; Goodgame, D. M. L.; Holm, R. H. *J. Am. Chem. Soc.* **1961**, *83*, 1780. (d) Cotton, F. A.; Goodgame, D. M. L.; Goodgame, M. *J. Am. Chem. Soc.* **1961**, *83*, 4690. (e) Cotton, F. A.; Holm, R. H. *J. Chem. Phys.* **1959**, *31*, 788. (f) Goodgame, D. M. L.; Goodgame, M. *Inorg. Chem.* **1965**, *4*, 139. (g) Holm, R. H.; Cotton, F. A. *J. Chem. Phys.* **1960**, *32*, 1168. (h) Bressan, M.; Corain, B.; Rigo, P.; Turco, A. *Inorg. Chem.* **1970**, *9*, 1733.

(16) Horrocks, W. D., Jr.; Van Hecke, G. R.; Hall, D. D. *Inorg. Chem.* **1967**, *6*, 694.

(17) (a) Ellermann, J.; Gruber, W. H. *Z. Anorg. Allg. Chem.* **1970**, *364*, 55. (b) Bianchini, C.; Meli, A.; Orlandini, A.; Sacconi, L. *J. Organomet. Chem.* **1981**, *209*, 219.

Scheme 2. Solution Equilibrium of the Isomers **2** and **3**

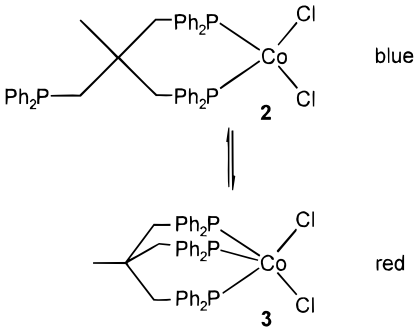

complexes[20] and have been proposed in catalytic cycles and stoichiometric reactions involving triphos complexes of Rh^{I}, Ir^{I}, and Rh^{III}.[21]

Spin-Crossover Equilibrium. Cooling a solution of **2** in THF results in a reversible color change from blue over violet to red suggesting that the isomeric complex **3** is formed. The color change can be monitored by UV/vis spectroscopy (Figure 4). The absorption bands of the blue complex **2** at 591, 640, and 738 nm gradually decrease while simultaneously the bands of the red species **3** at 553 and 945 nm gain intensity. The observation of three isosbestic points at 582, 770, and 1256 nm shows that the color change is associated with a simple equilibrium between two species without accumulation of a long-living intermediate (Scheme 2).

Additionally the spectra recorded at the extremes of the temperature range studied do not show large changes so the reaction appears to be almost complete within 160 K. From simple simulations of the electronic spectra at various temperatures the corresponding equilibrium concentrations of the two complexes **2** and **3** are estimated. The analysis of this temperature dependence yields the following thermodynamic parameters for the reaction **2** → **3** depicted in Scheme 2: $\Delta H = -19 \pm 4$ kJ mol^{-1}, $\Delta S = -84 \pm 8$ J mol^{-1} K^{-1}. The quite large errors are due to the inaccuracy of the simulation procedure.

As the two isomers do not only differ in their optical properties but also in their spin-state, the isomerization can also be followed by measuring the solution magnetic moment at different temperatures (Figure 5). The magnetic moment of 4.0 μ_B at 318 K gradually drops to 2.0 μ_B at 178 K (Figure 5). This variation of the magnetic moment is reversible (Figure 5: filled and hollow circles, respectively). The analysis of the temperature dependence is based on the expression

$$K = \frac{c(\mathbf{3})}{c(\mathbf{2})} = \frac{\mu_{\mathrm{eff}}{}^2 - \mu(\mathbf{2})^2}{\mu(\mathbf{3})^2 - \mu_{\mathrm{eff}}{}^2}$$

with $\mu(\mathbf{2}) = 4.1\ \mu_B$ and $\mu(\mathbf{3}) = 1.9\ \mu_B$ yielding $\Delta H = -21 \pm 3$ kJ mol^{-1} and $\Delta S = -85 \pm 6$ J mol^{-1} K^{-1}, which is in excellent agreement with the results obtained from the UV/vis spectroscopic experiment. The entropy change usually is interpreted as originating from the change of spin-multiplicity and the change of vibrational freedom. The spin-only term ΔS_{spin} (neglecting orbital contributions) for Co^{II} compounds ($S = {}^3/_2 \rightarrow S = {}^1/_2$) is evaluated as -5.8 J mol^{-1} K^{-1}.[22] The approximately 15 times larger entropy variation in the present spin-crossover system is certainly largely due to the dramatic loss of rotational and vibrational degrees of freedom of the coordinated phosphorus arm of the triphos ligand in **3**. Entropy variations in Co^{II} spin-crossover systems without detaching ligand arms lie in the range of -6 to -30 J mol^{-1} K^{-1}. Enthalpic changes in the order of <1 to -7 kJ mol^{-1} were found in spin-crossover compounds without ligand dissociation;[23] -14 to -17 kJ mol^{-1} were measured in systems with nitrogen donor atom dissociation.[24] The ΔH value of -20 kJ mol^{-1} in the present system therefore additionally supports the dissociative process involving one phosphorus arm of the triphos ligand.

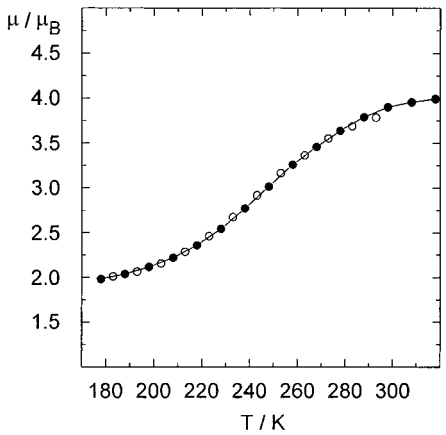

Figure 5. Magnetic moment of **2** in THF (●, cooling; ○, heating).

The equilibrium (Scheme 2) is not only influenced by temperature but also by the choice of solvent. A methylene chloride solution[25] at room temperature appears red suggesting the sole existence of **3**. In fact the UV/vis spectrum shows a mixture of both isomers (Table 4) and the magnetic moment in CH_2Cl_2 (Table 3) is somewhat higher than expected for pure **3**. A similar UV/vis spectrum is observed in ethanol and $CHCl_3$. Benzene, toluene, acetone, and dioxane yield blue solutions at room temperature, the red species **3** being present only in small amounts. At present it is not clear why these solvents stabilize either the red (**3**) or the blue species (**2**).

Dimer/Monomer Conversion. The monomeric species **2** can easily be converted into the dinuclear complexes **1**$(X)_2$ by adding chloride-abstracting reagents such as $NaBPh_4$, $NaPF_6$, or $NaBF_4$ (Scheme 3), involving a color change from blue to red. The compounds **1**$(BPh_4)_2$ (vide supra) and **1**$(PF_6)_2$ can easily be isolated (see Experimental Section). Adding chloride ions to solutions of either **1**$(BPh_4)_2$ or **1**$(PF_6)_2$ in THF in the

(18) (a) Blake, A. J.; Gould, R. O.; Halcrow, M. A.; Schröder, M. *J. Chem. Soc. Dalton Trans.* **1993**, 2909. (b) Bianchini, C.; Meli, A.; Scapacci, G. *Organometallics* **1985**, *4*, 264. (c) Reinhard, G.; Soltek, R.; Huttner, G.; Barth, A.; Walter, O.; Zsolnai, L. *Chem. Ber.* **1996**, *129*, 97.

(19) Lin, S. C.; Cheng, C. P.; Lee, T.-Y.; Lee, T.-J.; Peng, S.-M. *Acta Crystallogr.* **1986**, *C42*, 1733.

(20) Brandt, K.; Sheldrick, W. S. *Chem. Ber.* **1996**, *129*, 1199.

(21) (a) Hauger, B. E.; Huffman, J. C.; Caulton, K. G. *Organometallics* **1996**, *15*, 1856. (b) Siegl, W. O.; Lapporte, S. J.; Collman, J. P. *Inorg. Chem.* **1971**, *10*, 2158. (c) Ott, J.; Venanzi, L. M.; Ghilardi, C. A.; Midollini, S.; Orlandini, A. *J. Organomet. Chem.* **1985**, *291*, 89. (d) Thaler, E. G.; Folting, K.; Caulton, K. G. *J. Am. Chem. Soc.* **1990**, *112*, 2664. (e) Johnston, G. G.; Baird, M. C. *J. Chem. Soc. Chem. Commun.* **1989**, 1008. (f) Thaler, E. G.; Caulton, K. G. *Organometallics* **1990**, *9*, 1871. (g) Rauscher, D. J.; Thaler, E. G.; Huffman, J. C.; Caulton, K. G. *Organometallics* **1991**, *10*, 2209.

(22) Kahn, O. *Molecular Magnetism*; VCH Verlagsgesellschaft: Weinheim, Germany, 1993.

(23) (a) Thuéry, P.; Zarembowitch, J. *Inorg. Chem.* **1986**, *25*, 2001. (b) Zarembowitch, J. *New J. Chem.* **1992**, *16*, 255. (c) Everett, G. W.; Holm, R. H. *J. Am. Chem. Soc.* **1966**, *88*, 2442. (d) Everett, G. W.; Holm, R. H. *Inorg. Chem.* **1968**, *7*, 776. (e) Wolny, J. A.; Rudolf, M. F.; Ciunik, Z.; Gatner, K.; Wolowiec, S. *J. Chem. Soc. Dalton Trans.* **1993**, 1661.

(24) (a) Bianchini, A.; Calabresi, C.; Ghilardi, C. A.; Orioli, P. L.; Sacconi, L. *J. Chem. Soc., Dalton Trans.* **1973**, 1383. (b) Morassi, R.; Mani, F.; Sacconi, L. *Inorg. Chem.* **1973**, *12*, 1246. (c) Gatteschi, D.; Ghilardi, C. A.; Orlandini, A.; Sacconi, L. *Inorg. Chem.* **1978**, *17*, 3023. (d) Kelly, W. S. J.; Ford, G. H.; Nelson, S. M. *J. Chem. Soc. A* **1971**, 388. (e) Dahlhoff, W. V.; Nelson, S. M. *J. Chem. Soc. A* **1971**, 2184.

(25) Possible traces of HCl present in CH_2Cl_2 were removed by filtration over basic alumina.

Scheme 3. Conversions between the Mononuclear and Dinuclear Species **2** and $\mathbf{1}^{2+}$

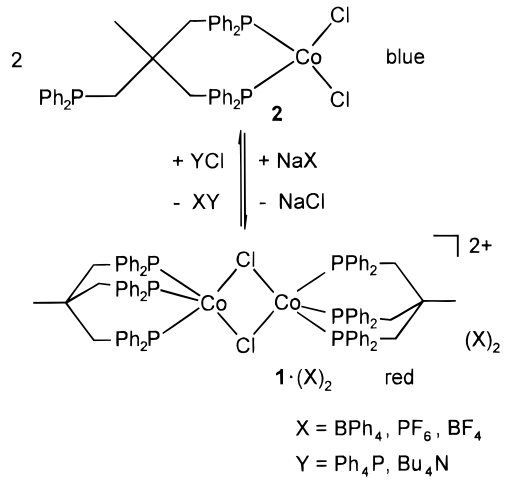

form of their tetraphenylphosphonium or tetrabutylammonium salts again restores the blue color of **2**. So in addition to the easy dissociation of one phosphorus donor atom one chloride ion can be removed leading to the formation of highly unsaturated 15 VE species $[(\text{triphos})\text{CoCl}]^+$ which dimerize in order to gain stable 17 VE configurations (in the absence of other potential ligands; vide infra).

Reaction with Lewis Acids. The products obtained by reactions of **2** with MCl_2 (M = Zn, Fe, Co) have all the same empirical formula of $[(\text{triphos})\text{CoMCl}_4]$, but their solid-state structures depend on the Lewis acid strength of the metal chloride employed and the isolation procedure, especially the solvent used. The stronger Lewis acid $ZnCl_2$ abstracts one chloride ion (presumably assisted by the coordination of the dangling phosphane group of the triphos ligand present in **2**) to give the reactive 15 VE species $[(\text{triphos})\text{CoCl}]^+$ and a solvated $[ZnCl_3(THF)_x]^-$ fragment (Scheme 4, left pathway). Both fragments dimerize to give $[(\text{triphos})_2Co_2Cl_2]^{2+}$ and $(Zn_2Cl_6)^{2-}$. The reaction is accompanied by a color change from blue (**2**) to red (the dinuclear complex $\mathbf{1}^{2+}$). Crystals of the CH_2Cl_2 solvate of $\mathbf{1}(Zn_2Cl_6)$ can be obtained by recrystallization from CH_2Cl_2/Et_2O (Tables 1 and 5). However, solutions of pure $\mathbf{1}(Zn_2Cl_6)$ in CH_2Cl_2 do not exhibit the expected conductivity of a 2:2 electrolyte, the conductivity being much lower (Table 3). Additionally the UV/vis spectrum shows besides the expected absorptions of the dinuclear cation $\mathbf{1}^{2+}$ (Table 4) bands attributable to the blue, nonionic high-spin compound **2**. Therefore in solution several species must be present: the dication $\mathbf{1}^{2+}$, the uncharged red complex **3** (with bands overlapping those of $\mathbf{1}^{2+}$), its isomer **2**, and presumably a loosely bound associate of **3** and $ZnCl_2(THF)_x$ (Scheme 4, left pathway).

In one attempt to recrystallize **3** from a THF solution, in addition to a large amount of **3** (red needles) a few blue crystals of $\mathbf{1}(CoCl_3THF)_2$ as a THF solvate were obtained (Scheme 4, left pathway). Here—as in the case of $ZnCl_2$—a chloride transfer from the starting complex **2** to an additional $CoCl_2$ fragment has occurred to give the dimer $[(\text{triphos})_2Co_2Cl_2]^{2+}$ ($\mathbf{1}^{2+}$) and $(CoCl_3THF)^-$ (Tables 1 and 5).

These observations prompted us to investigate the reaction of **2** with other Lewis acids such as $FeCl_2$ and $CoCl_2$ in different solvents (Scheme 4, right pathway). Cobalt dichloride precipitates a violet solid of the empirical formula $[(\text{triphos})Co_2Cl_4]$ (**6**) from THF solutions of **2**; iron dichloride yields a red solution (**5**). Both compounds can be recrystallized from CH_2Cl_2/Et_2O. The solid-state structures of both adducts are determined by X-ray diffraction methods. As both crystals are isomorphous, only the structure of the cobalt adduct (**6**) is depicted in Figure 6. In both cases all three phosphorus atoms as well as two chlorides are coordinated to the cobalt center. The additional

Scheme 4. Reaction of **2** with Lewis Acids

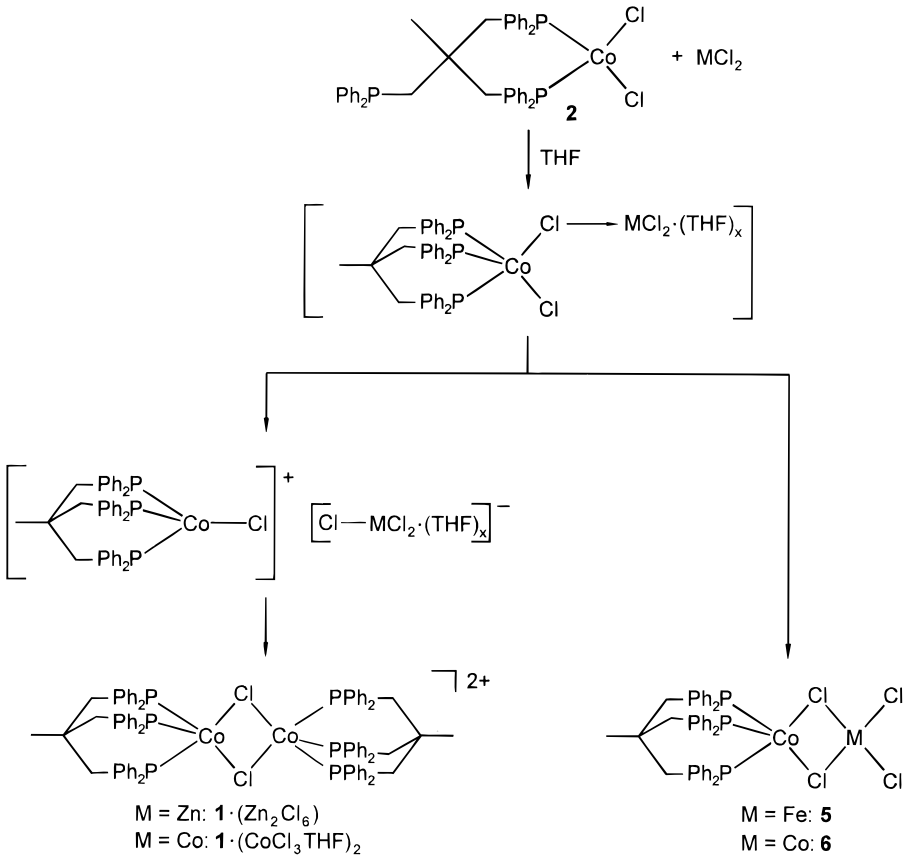

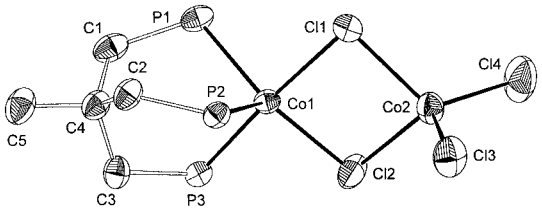

Figure 6. ZORTEP view of **6**.[45]

MCl_2 fragment (**5**, M = Fe; **6**, M = Co) is coordinated to the two chlorides forming a dinuclear complex. The dinuclear complexes can also be thought of as being composed of a $[(triphos)Co]^{2+}$ fragment and a chelating MCl_4^{2-} ion.[32] Obviously the coordination of the MCl_2 fragment at the $[(triphos)CoCl_2]$ fragment in the solid state (with CH_2Cl_2 solvate molecules) is favored over the chloride abstraction (to form MCl_4^{2-} and $[(triphos)_2Co_2Cl_2]^{2+}$, $\mathbf{1}^{2+}$). In solution, however, similar to the $ZnCl_2$ case also ionic species and Co^{II} high-spin species must be present (as implied by conductivity and UV/vis data, Tables 3 and 4). The solid-state structures of **5** and **6** might therefore be considered as "snapshots" or "frozen transition states"[26] of the chloride abstraction reaction which is favored with $ZnCl_2$, $CoCl_2$ in THF, $NaBPh_4$, $NaPF_6$, and $NaBF_4$ (vide supra).

Solid State Structures. Five-coordinate complexes with the triphos ligand cannot adopt one of the possible ideal structures of five-coordination, the square pyramid (SP, C_{4v}) or the trigonal bipyramid (TBP, D_{3h}), owing to the ligand-imposed 90° P−M−P angles. But in most cases it is possible to assign a distorted SP or TBP structure.[27] Additionally it is often observed that in solution two species which only differ in their stereochemistry exist or that in solution rapid equilibria between these species occur.[1de,14cd,28] The two limiting stereochemistries of a five-coordinate complex have been discovered in the solid state for the $[(dppe)_2CoCl]SnCl_3$ complex (dppe = 1,2-bis-((diphenylphosphino))ethane).[29] In the case of the centrosymmetric dications $\mathbf{1}^{2+}$ isolated as the $(BPh_4)^-$, the $(Zn_2Cl_6)^{2-}$, or the $(CoCl_3THF)^-$ salt a distorted SP structure with P2 in the apical position is observed in $\mathbf{1}(BPh_4)_2$ (Figure 1) while distorted TBP structures with P3 and Cl1 in the apical positions are found in $\mathbf{1}(Zn_2Cl_6)$ and $\mathbf{1}(CoCl_3THF)_2$ (Table 5). Neither the counterions[30] nor the solvate molecules have short contacts with the dications in the crystal lattice. It is concluded that both structures represent local minima on the energy hypersurface of the TBP/SP isomerization pathway supporting the previously given interpretation of solution EPR spectra of $[(triphos)Co^{II}L_2]$ complexes which clearly show the presence of two species.[1d,e,14c,d,28] The dications also show small differences in the planar Co−Cl−Co−Cl ring system: The Cl−Co−Cl angle increases on going from $\mathbf{1}(BPh_4)_2$ to $\mathbf{1}(Zn_2Cl_6)$ or to $\mathbf{1}(CoCl_3THF)_2$ while the Co−Cl−Co angle decreases resulting in smaller Co···Co distances in $\mathbf{1}(Zn_2Cl_6)$ and $\mathbf{1}(CoCl_3THF)_2$ (Table 5).

The mononuclear low-spin complex **3** (Figure 2) exhibits a distorted TBP geometry with P3 and Cl1 occupying axial coordination sites (Table 5). The Co−Cl distances are significantly shorter than those of the bridging chlorides found in the dinuclear complexes $\mathbf{1}^{2+}$. Also the Cl−Co−Cl angle is expanded in **3**; both observations can be attributed to the strain occurring in the Co−Cl−Co−Cl ring system of the dinuclear complexes.

Table 5. Selected Bond Lengths (Å) and Angles (deg) for $\mathbf{1}(BPh_4)_2$, **3**, **4**, $\mathbf{1}(Zn_2Cl_6)$, and $\mathbf{1}(CoCl_3THF)_2$

	$\mathbf{1}(BPh_4)_2$	**3**	**4**	$\mathbf{1}(Zn_2Cl_6)$	$\mathbf{1}(CoCl_3THF)_2$
Co1−P1	2.221(1)	2.256(4)	2.329(1)	2.282(1)	2.238(1)
Co1−P2	2.312(1)	2.234(4)	2.352(1)	2.249(1)	2.292(1)
Co1−P3	2.247(1)	2.196(4)		2.215(1)	2.223(1)
Co1−Cl1	2.302(1)	2.252(3)	2.234(1)	2.296(1)	2.290(1)
Co1−Cl2	2.296(1)	2.268(4)	2.216(1)	2.288(1)	2.294(1)
Co1···Co2	3.52			3.46	3.47
P1−Co1−P2	89.62(5)	96.3(1)	95.79(4)	95.64(4)	96.58(4)
P1−Co1−P3	88.43(5)	89.1(1)		86.92(4)	86.47(4)
P2−Co1−P3	93.86(5)	88.6(1)		89.57(4)	88.95(4)
P1−Co1−Cl1	90.83(5)	94.5(1)	101.75(4)	93.97(4)	93.90(4)
P1−Co1−Cl2	167.94(6)	134.6(2)	118.95(5)	149.22(4)	153.19(4)
P2−Co1−Cl1	117.94(6)	91.2(2)	102.36(5)	97.90(4)	97.41(4)
P2−Co1−Cl2	101.62(6)	129.0(2)	115.69(5)	115.14(4)	110.19(4)
P3−Co1−Cl1	148.19(6)	176.4(2)		172.35(4)	173.53(4)
P3−Co1−Cl2	95.09(5)	88.5(1)		93.34(4)	95.14(4)
Cl1−Co1−Cl2	80.00(5)	88.8(1)	118.65(5)	82.01(4)	81.63(4)
Co1−Cl1−Co2	99.99(5)			97.99(4)	98.37(4)

Comparing the five-coordinate low-spin complex **3** (Figure 2) with the pseudotetrahedral high-spin complex **4** (Figure 3) shows that the Co−Cl bond lengths are *shorter* in the high-spin compound (Table 5) which is unexpected from electronic considerations alone but can be rationalized in terms of the lower coordination number of **4**. The Co−P distances on the other hand are 0.02−0.05 Å larger in **4** than in **3** as expected. The lower coordination number of **4** also allows the Cl−Co−Cl angle to expand from 89° in **3** to 119° in **4** (Table 5).

The heterodinuclear complexes **5** and **6** (Figure 6) exhibit—analogous to the $\mathbf{1}^{2+}$ dications—a Co−Cl−M−Cl four-membered ring system which is planar in the dications $\mathbf{1}^{2+}$ (angles between the two Cl−Co−Cl planes: 180°) but folded in **5** and **6** (angles between the Cl−Co−Cl and Cl−M−Cl plane: 162°) resulting in a butterfly geometry. Also the angles within the ring systems are different, the Cl−Co−Cl angle in **5** and **6** being larger and the Co−Cl−M angle ($\mathbf{1}^{2+}$, M = Co; **5**, M = Fe; **6**, M = Co) being smaller. The distances between the metal of the [(triphos)Co] fragment and the bridging chloride remain almost constant in all dinuclear complexes (Tables 5 and 6). As the crystals of **5** and **6** are isomorphous (Tables 1 and 2), they do not differ in their overall geometry especially

(26) McAuliffe, C. A.; Godfrey, S. M.; Mackie, A. G.; Pritchard, R. G. *Angew. Chem.* **1992**, *104*, 932; *Angew. Chem., Int. Ed. Engl.* **1992**, *31*, 919.

(27) (a) Wood, J. S. *Prog. Inorg. Chem.* **1972**, *16*, 227. (b) Furlani, C. *Coord. Chem. Rev.* **1968**, *3*, 141. (c) Orioli, P. L. *Coord. Chem. Rev.* **1971**, *6*, 285. (d) Beyreuther, S.; Hunger, J.; Huttner, G.; Mann, S.; Zsolnai, L. *Chem. Ber.* **1996**, *129*, 745.

(28) Körner, V.; Huttner, G.; Zsolnai, L.; Büchner, M.; Jacobi, A.; Günauer, D. *Chem. Ber.* **1996**, *129*, 1587.

(29) (a) Stalick, J. K.; Corfield, P. W. R.; Meek, D. W. *J. Am. Chem. Soc.* **1972**, *94*, 6194. (b) Stalick, J. K.; Meek, D. W. *J. Chem. Soc. Chem. Commun.* **1972**, 630.

(30) The $(Zn_2Cl_6)^{2-}$ dianion of $\mathbf{1}(Zn_2Cl_6)$ consists of two edge-sharing tetrahedra, essentially identical to previously reported hexachlorodizincates. Relevant bond lengths (Å) and angles (deg): Zn1−Cl2 2.217(1), Zn1−Cl3 2.208(1), Zn1−Cl4 2.343(1), Zn1−Cl4A 2.335(1), Cl2−Zn1−Cl3 113.99(5), Cl2−Zn1−Cl4 113.70(5), Cl2−Zn1−Cl4A 110.64(5), Cl3−Zn1−Cl4 113.82(5), Cl3−Zn1−Cl4A 111.66(6), Cl4−Zn1−Cl4A 90.83(4). (a) Wilhelm, J. H.; Müller, U. *Z. Naturforsch.* **1989**, *44b*, 1037. (b) Bremer, J.; Wegner, R.; Krebs, B. *Z. Anorg. Allg. Chem.* **1995**, *621*, 1123. (c) Bottomley, F.; Karslioglu, S. *Organometallics* **1992**, *11*, 326. (d) Doxsee, K. M.; Hagadorn, J. R.; Weakley, T. J. R. *Inorg. Chem.* **1994**, *33*, 2600. (e) Cotton, F. A.; Duraj, S. A.; Roth, W. J. *Inorg. Chem.* **1985**, *24*, 913. (f) Bouma, R. J.; Teuben, J. H.; Beukema, W. R.; Bansemer, R. L.; Huffman, J. C.; Caulton, K. G. *Inorg. Chem.* **1984**, *23*, 2715. (g) Sekutowsky, D. G.; Stucky, G. D. *Inorg. Chem.* **1975**, *14*, 2192. The $(CoCl_3THF)^-$ anion of $\mathbf{1}(CoCl_3THF)_2$ is pseudotetrahedral, essentially identical to previously reported trichloro(tetrahydrofuran)cobaltates(II). Relevant bond lengths (Å) and angles (deg): Co2−Cl2 2.244(1), Co2−Cl3 2.242(1), Co2−Cl4 2.234(1), Co2−O1 2.038(3), Cl2−Co2−Cl3 114.82(7), Cl2−Co2−Cl4 110.53(5), Cl2−Co2−O1 103.5(1), Cl3−Co2−Cl4 118.40(7), Cl3−Co2−O1 102.4(1), Cl4−Co2−O1 105.1(1). (a) Fenske, D.; Ohmer, J.; Merzweiler, K. *Z. Naturforsch.* **1987**, *42b*, 803. (b) Fenske, D.; Hachgenei, J.; Ohmer, J. *Angew. Chem.* **1985**, *97*, 684; *Angew. Chem., Int. Ed. Engl.* **1985**, *24*, 706. (c) Döring, M.; Görls, H.; Uhlig, E.; Brodersen, K.; Dahlenburg, L.; Wolski, A. *Z. Anorg. Allg. Chem.* **1992**, *614*, 65. (d) Solari, E.; Corazza, F.; Floriani, C.; Chiesi-Villa, A.; Guastini, C. *J. Chem. Soc., Dalton Trans.* **1990**, 1345.

Table 6. Selected Bond Lengths (Å) and Angles (deg) for **5** and **6**

	5[a]	**6**[b]
Co1−P1	2.255(2)	2.257(1)
Co1−P2	2.274(2)	2.270(1)
Co1−P3	2.198(2)	2.201(1)
Co1−Cl1	2.283(2)	2.297(1)
Co1−Cl2	2.297(2)	2.310(1)
Co1···M	3.47	3.36
M−Cl1	2.392(2)	2.322(1)
M−Cl2	2.384(2)	2.320(1)
M−Cl3	2.230(2)	2.219(1)
M−Cl4	2.221(2)	2.212(2)
P1−Co1−P2	92.22(8)	92.18(5)
P1−Co1−P3	88.29(8)	88.48(5)
P2−Co1−P3	90.70(8)	90.75(5)
P1−Co1−Cl1	93.52(8)	93.32(5)
P1−Co1−Cl2	148.11(8)	146.98(6)
P2−Co1−Cl1	99.08(8)	98.10(5)
P2−Co1−Cl2	119.52(8)	120.67(5)
P3−Co1−Cl1	169.96(9)	170.89(6)
P3−Co1−Cl2	88.41(7)	87.93(5)
Cl1−Co1−Cl2	84.85(8)	85.70(5)
Co1−Cl1−M	95.83(8)	93.46(5)
Co1−Cl2−M	95.67(8)	93.18(5)
Cl1−M−Cl2	80.64(7)	84.90(5)
Cl1−M−Cl3	111.41(9)	111.28(6)
Cl1−M−Cl4	114.84(9)	117.06(6)
Cl2−M−Cl3	106.58(9)	108.64(6)
Cl2−M−Cl4	119.2(1)	117.72(7)
Cl3−M−Cl4	118.2(1)	113.99(6)

[a] M = Fe1. [b] M = Co2.

within the [(triphos)Co] fragment. The M−Cl distances (**5**, M = Fe; **6**, M = Co), however, are significantly different, the Fe−Cl distances in **5** being larger than the Co−Cl distances in **6** in spite of the similar ionic radii[31] of Fe^{II} and Co^{II}. This is expected from simple ligand field arguments: Removing a bonding electron (e-orbital set) from a tetrahedral d^7 complex (Co^{II}) to form a tetrahedral d^6 complex (Fe^{II}) should weaken the M−Cl bonds.[32ab]

Solid-State Magnetism. The magnetic behavior of **3**, **1**(Zn_2Cl_6), **5**, and **6** in the solid state was measured in the temperature range from 5 to 300 K. **3** exhibits normal Curie−Weiss behavior ($\Theta = 3.2$ K) with a temperature-independent magnetic moment of 2.1 μ_B indicating a low-spin d^7 configuration with the ususal orbital contribution raising the moment above the spin-only value of 1.73 μ_B. As expected, compound **3** shows no high-spin/low-spin transition in the solid state as the transition involves large structural changes (vide supra).

The symmetrical dinuclear complex **1**(Zn_2Cl_6) has a room-temperature magnetic moment of 2.5 μ_B per dinuclear unit which is lower than expected (2.6−3.1 μ_B) for two noninteracting $S = {}^1/_2$ spin systems and it decreases with temperature. The magnetic susceptibility initially increases with temperature, and after reaching a broad maximum around 190 K, it decreases toward 50 K. This temperature dependence can be related to a single exchange term in the Hamiltonian of the form $H = -2JS_AS_B$, with $S_A = S_B = {}^1/_2$.[22] A least-squares fitting over the observed susceptibilities with a fixed g-value of 2.11 yields $J = -109$ cm^{-1} (the fit does not improve significantly with a varying g-factor; $g = 2.23$; $J = -116$ cm^{-1}). This quite strong antiferromagnetic exchange interaction has also been observed for **1**(BPh_4)$_2$ ($g = 2.38$, $J = -117$ cm^{-1}, measured between 90 and 300 K),[3] showing that indeed an intramolecular rather than an intermolecular interaction is operative.

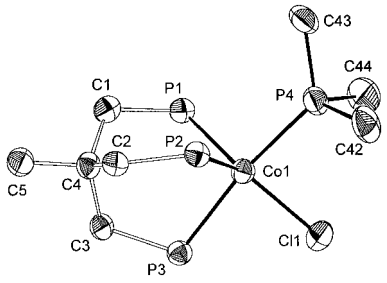

Figure 7. ZORTEP view of the cation of **8**(BPh_4).[45]

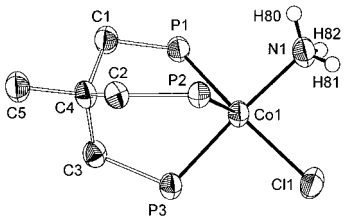

Figure 8. ZORTEP view of the cation of **9**(BPh_4).[45]

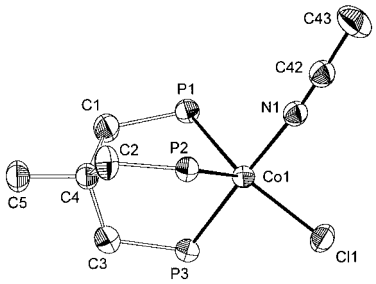

Figure 9. ZORTEP view of the cation of **10**(BPh_4).[45]

Both unsymmetrical dinuclear complexes **5** and **6** with a low-spin Co^{II} and a tetrahedral high-spin M^{II} center have a constant magnetic moment of 5.8 and 5.0 μ_B, respectively. The moments for noninteracting spin-systems are expected to be 5.7−5.8 μ_B[32c] ($S_A = {}^1/_2$; $S_B = 2$) and 4.9−5.1 μ_B[15d,e,g] ($S_A = {}^1/_2$; $S_B = {}^3/_2$), respectively. The linearity of the χ^{-1} vs T plots as well as the values of the magnetic moment indicate a vanishing interaction between the two spin-carriers in **5** and **6**.

Reaction with Lewis Bases. Both hard and soft Lewis bases L (L = CO, PMe_3, NH_3, and CH_3CN) react with **2** in THF in the presence of $NaBPh_4$ to give the chloride substitution product $[(triphos)CoCl(L)]^+$ (Scheme 5). The carbonyl derivative **7**(BPh_4) was previously prepared by addition of CO to **1**(BPh_4)$_2$.[1g] Therefore **7**(BPh_4) is only characterized by its IR- and UV/vis spectra which match the reported ones.[1g] The constitution of the complexes **8**(BPh_4)−**10**(BPh_4) is determined by elemental analyses, UV/vis, EPR, and IR spectra, conductivity, and magnetic susceptibility measurements. The data are fully consistent with the formulation of five-coordinate, low-spin complexes which behave as 1:1 electrolytes (Tables 3 and 4). X-ray structure determinations confirm these assignments (Figures 7−9).

In spite of the fact that both hard and soft Lewis bases yield the substitution product, the reaction mechanisms appear to be different: The soft π-acceptor ligands carbon monoxide and trimethylphosphine already react with **2** in the absence of the chloride abstracting reagent $NaBPh_4$ (as shown by UV/vis spectroscopy) while the σ-donor ligands ammonia and acetonitrile—even if added in large excess—do not react with **2**. On addition of $NaBPh_4$, however, the reaction proceeds within seconds (see Experimental Section). It is therefore assumed that CO and PMe_3 directly add to the tetrahedral [(η^2-triphos)$CoCl_2$] complex **2** to give a five-coordinate intermediate which—probably activated by the trans-effect of CO, PMe_3, or

(31) Holleman, A. F.; Wiberg, E. *Textbook of Inorganic Chemistry*; Walter de Gruyter: Berlin, New York, 1985.
(32) (a) Lauher, J. W.; Ibers, J. A. *Inorg. Chem.* **1975**, *14*, 348. (b) Toan, T.; Dahl, L. F. *J. Am. Chem. Soc.* **1971**, *93*, 2654. (c) Clark, R. J. H.; Nyholm, R. S.; Taylor, F. B. *J. Chem. Soc. A* **1967**, 1802.

Scheme 5. Reaction of **2** with Lewis Bases

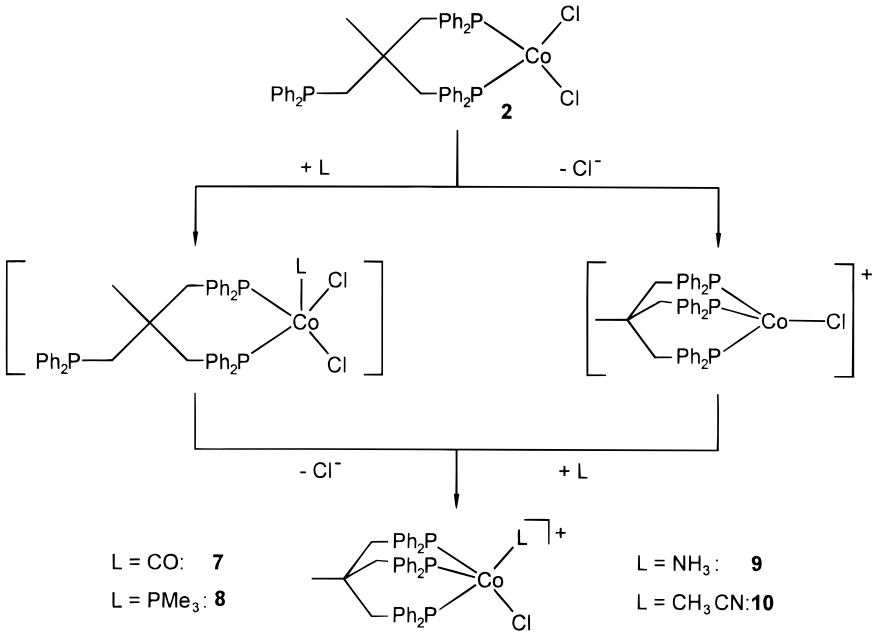

Table 7. Selected Bond Lengths (Å) and Angles (deg) for **8**(BPh_4), **9**(BPh_4), and **10**(BPh_4)

	8(BPh_4)[a]	**9**(BPh_4)[b]	**10**(BPh_4)[b]
Co1−P1	2.251(1)	2.242(1)	2.250(1)
Co1−P2	2.277(2)	2.280(1)	2.261(1)
Co1−P3	2.296(1)	2.208(1)	2.205(1)
Co1−Cl1	2.264(1)	2.254(1)	2.251(1)
Co1−X	2.268(1)	2.008(4)	1.914(2)
P1−Co1−P2	95.67(4)	94.65(5)	93.48(3)
P1−Co1−P3	89.31(5)	89.88(5)	88.54(3)
P2−Co1−P3	88.17(5)	87.50(5)	91.65(3)
P1−Co−X	97.59(5)	90.6(1)	91.48(6)
P2−Co−X	95.83(5)	98.9(1)	92.00(7)
P3−Co−X	171.62(4)	173.5(1)	176.34(6)
Cl1−Co−P1	137.55(5)	150.83(6)	142.63(3)
Cl1−Co−P2	126.63(5)	114.51(5)	123.85(3)
Cl1−Co−P3	88.77(5)	91.20(5)	88.83(3)
Cl1−Co−X	82.94(5)	85.3(1)	88.94(6)

[a] X = P4. [b] X = N1.

the phosphine group of the triphos ligand—loses one chloride ion (Scheme 5, left pathway, A mechanism). A reversible addition of CO to tetrahedral $Co(PR_3)_2X_2$ complexes to form five-coordinate complexes of the type $Co(PR_3)_2(CO)X_2$ has previously been observed.[15h] The N-donor ligands (NH_3, CH_3CN) obviously are not able to expel the chloride ion; hence, activation by a Lewis acid is necessary: The $NaBPh_4$ abstracts one chloride ion to form the unsaturated species $[(triphos)CoCl]^+$ (vide supra) which adds the ligand L (Scheme 5, right pathway, D mechanism). Also interesting to note is that the complexes **9**(BPh_4) and **10**(BPh_4) slowly lose their ligand L both in solution and in the solid state to give the dinuclear complex **1**$(BPh_4)_2$ (see Experimental Section) and that they are highly sensitive toward dioxygen while **8**(BPh_4) is stable toward dissociation and inert against dioxygen even for months.

In the solid state the cations of **8**(BPh_4) (Figure 7), **9**(BPh_4) (Figure 8), and **10**(BPh_4) (Figure 9) adopt a distorted TBP with P3/P4 ($\mathbf{8}^+$) and P3/N1 ($\mathbf{9}^+$, $\mathbf{10}^+$) occupying axial coordination sites, respectively (Table 7). The Co−Cl bond lengths are almost identical and also similar to those found in **3**. The coordinated acetonitrile in $\mathbf{10}^+$ exhibits geometric parameters similar to those found in the bis(acetonitrile) complex $[(triphos)Co(NCCH_3)_2]^{2+}$.[14e] The Co−N distance in $\mathbf{9}^+$ compares with those found in other $[(triphos)Co(NH_2R)]^{x+}$ complexes.[14f,28] Remarkably the N···Cl distance of 2.89 Å is smaller than the sum of the van der Waals radii of 3.30 Å.[36] A short Cl···H−NH_2[33] contact is found (Cl1···H81 = 2.69 Å, all other Y···H−NH_2 distances being larger than 3 Å) which also falls significantly below the sum of the van der Waals radii of hydrogen and chlorine (3.00 Å).[36] Therefore a weak intramolecular hydrogen bond between Cl1 and H81 might be present. In unconstrained systems with intermolecular hydrogen bonds, Cl···H distances of 2.4−2.6 Å and an almost linear arrangement of the N−H···Cl moiety (found: 97°) are found.[34] The interaction is also observed in the IR spectrum of **9**(BPh_4): It shows more N−H stretching bands (see Experimental Section) than expected for a local C_{3v} symmetry around the nitrogen (A_1 + E), and two N−H absorptions are strongly shifted to lower wavenumbers (3248, 3197 cm^{-1}) indicative of a secondary interaction.[35] The same pattern of the N−H absorptions is observed in solution thereby excluding packing effects and lattice forces causing the splitting of the bands.

The different colors observed for **7**(BPh_4)−**8**(BPh_4) (green) and **9**(BPh_4)−**10**(BPh_4) (orange-brown) are due to the bathochromic shift (around 1000 cm^{-1}) of the $(e'')^4(e')^3 \rightarrow (e'')^4(e')^2(a_1')^1$ and $(e'')^4(e')^3 \rightarrow (e'')^3(e')^3(a_1')^1$ absorption bands (in idealized D_{3h} symmetry)[27a−c] on replacing the strong ligands CO or PMe_3 with nitrogen-donor ligands. The observed trend corresponds well to the order of the spectrochemical series[36] with CO > PMe_3 ≫ NH_3 ≈ CH_3CN.

Redox Chemistry. The cyclic voltammogram of **3** in CH_2Cl_2 is shown in Figure 10. **3** is reversibly oxidized at 335 mV

(33) The positions of the hydrogens of the NH_3 ligand (H80, H81, H82) have been obtained by a ΔF map and have been refined together with their thermal parameters. Relevant bond lengths (Å) and angles (deg): N1−H80 0.93(5), N1−H81 0.79(5), N1−H82 0.91(6), Cl1···H80 3.77, Cl1···H81 2.69, Cl1···H82 3.05, H80−N1−H81 111(5), H80−N1−H82 109(4), H81−N1−H82 98(5), H80−N1−Co1 117(3), H81−N1−Co1 112(4), H82−N1−Co1 109(3). No short *intermolecular* contacts have been found.

(34) (a) Kollman, P. A.; Allen, L. C. *Chem. Rev.* **1972**, *72*, 283. (b) Scnalon, L. G.; Tsao, Y.-Y.; Toman, K.; Cummings, S. C.; Meek, D. W. *Inorg. Chem.* **1982**, *21*, 2707. (c) Buckingham, D. A.; Edwards, J. D.; McLaughlin, G. M. *Inorg. Chem.* **1982**, *21*, 2770.

(35) (a) Hesse, M.; Meier, H.; Zeeh, B. *Spectroscopic Methods in Organic Chemistry*; Georg Thieme Verlag: Stuttgart, New York, 1991. (b) Joesten, M. D. *J. Chem. Educ.* **1982**, *59*, 362. (c) For the cation $[CoCl(H_2N(CH_2)_3P(Ph)(CH_2)_3P(Ph)(CH_2)_3NH_2)]^+$, the N−H stretching vibrations (hydrogen-bonded) were observed at 3240 and 3190 cm^{-1}.[34b]

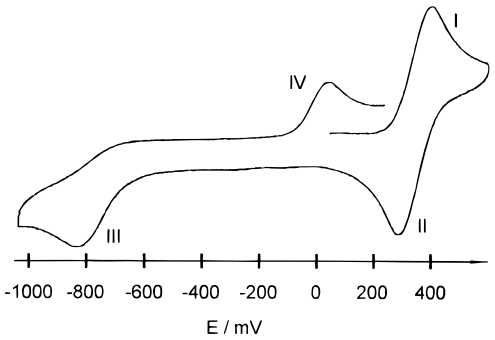

Figure 10. Cyclic voltammogram of **3** in CH_2Cl_2.

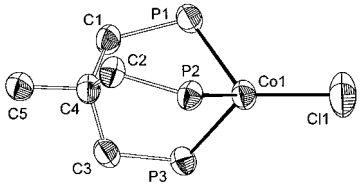

Figure 11. ZORTEP view of **11**.[45]

(Figure 10, I and II). An irreversible reduction wave is observed at −830 mV (Figure 10, III). The reduction product is at least partially re-oxidized in the reverse scan at +35 mV (Figure 10, IV). In the view of the known [(triphos)$Co^{I}Cl$] complex **11**[2] with cobalt having the oxidation state +I the interpretation of the reduction process is straighforward. At point III in the cyclic voltammogram [(triphos)$CoCl_2$] (**3**) undergoes a one-electron reduction of the metal center with a fast dissociation of one chloride ion. The current of the re-oxidation at point IV amounts to only approximately 70% of that of the reduction at point III—presumably due to diffusion processes of the reduction products **11** and chloride. Varying the scan speed up to 1000 mV/s does not alter this ratio significantly. The oxidation process at point I/II exhibits all features of a fully reversible electron transfer ($i_{pD}/i_{pA} = 1$; $i_{pA}/v^{1/2}$ = constant with $v = 50-1000$ mV/s; $\Delta E = 110$ mV which is smaller than that of Fc/Fc^+ (150 mV) under these conditions) allowing for an easy interpretation: [(triphos)$Co^{II}Cl_2$] **3** is oxidized to the Co^{III} derivative $\mathbf{12}^+$ without major structural changes. To demonstrate that these interpretations are correct and that indeed [(triphos)Co^{I}] and [(triphos)Co^{III}] chlorides are formed, we investigated preparative syntheses of these species for further characterization.

The Co^{I} complex can be prepared by reduction of **2** (or **3**) with $NaBH_4$,[2a] BH_3·THF,[37] or triethylamine.[6] The reduction with borane proved to be the most easy and clean reaction (Scheme 6). As borane is a strong Lewis acid and in view of the observed reactivity of [(triphos)$CoCl_2$] toward Lewis acids to yield the unsaturated species $[(triphos)CoCl]^+$ which reacts with almost any nucleophile present in solution, it is proposed that a [(triphos)Co(Cl)(H)] intermediate is formed which undergoes reductive dihydrogen elimination. This suggestion is supported—albeit not proved—by the observation that significant amounts of the known hydride complex [(triphos)Co-$(\mu\text{-H})_3$Co(triphos)]$^+$ [38] (identified by its UV/vis spectrum) are formed if the reaction is carried out at low temperatures with large excess of reducing agent in a closed Schlenk tube. The reaction of [(triphos)$CoCl_2$] with triethylamine yields as the only

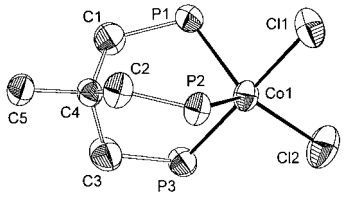

Figure 12. ZORTEP view of the cation of **12**(BCl_4).[45]

Scheme 6. Reduction of **2**

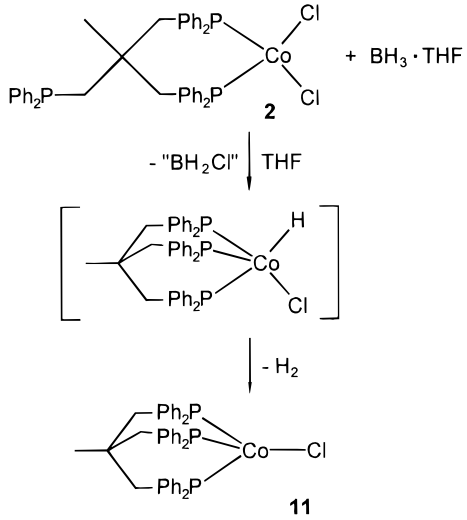

product detectable by UV/vis spectroscopy the Co^{I} complex **11**. The reaction pathway is currently investigated.

The four-coordinate structure of **11** is confirmed by an X-ray structural determination (Figure 11). The geometry around the metal is pseudotetrahedral with small P−Co−P angles around 90° due to the steric implications of the triphos ligand and larger P−Co−Cl angles around 120° (Table 8) which is typical for [(triphos)MX] complexes (M = Co, Ni, Cu; X = Cl, Br, I, NO, HCOO, BH_4, SO_2, CS_2).[2a,14f,39] Analytical and spectral data of **11** match those reported in the literature (Tables 3 and 4).[2]

Attempts to oxidize the 17 VE complex **3** to the 16 VE species $\mathbf{12}^+$ with $(NO)(BF_4)$, Ce^{IV} salts, tetrachloro-*p*-benzoquinone, chlorine, HCl/O_2, or $FeCl_3$ fail as mixtures of products or only decomposition products are obtained. The preparation of $\mathbf{12}^+$ is finally achieved by substitution of the catecholato ligand in $[(triphos)Co^{III}(cat)]^+$ complexes (cat = 1,2-dioxobenzene,[7] 4,5-(methylenedioxo)-1,2-dioxobenzene[1f]) with chloride ions provided by boron trichloride (Scheme 7) or by oxidation of **3** with $(Cp_2Fe)(BF_4)$. Certainly, the high affinity of boron toward oxygen donor atoms forming catechol chloroboronates[8a−c] (Scheme 7) is the driving force of the ligand-exchange reaction in analogy to the cleavage of aryl methyl ethers by boron halides.[8d,e] Compound $\mathbf{12}^+$ as a d^6-Co^{III} complex is diamagnetic and air-stable. The ^{31}P-NMR spectrum exhibits a single resonance for the three phosphorus atoms of the triphos ligand at 26.6 ppm consistent with a rapid intramolecular exchange of the phosphorus atoms as commonly found in five-coordinate triphos complexes.[1d−f,7,20,21c,d,21g,40] The ^{1}H- and ^{13}C-NMR

(36) Huheey, J. E. *Inorganic Chemistry*; Walter de Gruyter: Berlin, New York, 1988.

(37) The $NaBH_4$ present in commercial BH_3·THF solutions as stabilizer is *not* the reducing agent as bubbling inert gas through a BH_3·THF solution into the reaction Schlenk tube also leads to the reaction.

(38) Dapporto, P.; Midollini, S.; Sacconi, L. *Inorg. Chem.* **1975**, *14*, 1643.

(39) (a) Sernau, V.; Huttner, G.; Scherer, J.; Walter, O. *Chem. Ber.* **1996**, *129*, 243. (b) Dapporto, P.; Fallani, G.; Midollini, S.; Saconi, L. *J. Chem. Soc., Chem. Commun.* **1972**, 1161. (c) Dapporto, P.; Midollini, S.; Orlandini, A.; Saconi, L. *Inorg. Chem.* **1976**, *15*, 2768. (d) Bianchini, C.; Masi, D.; Mealli, C.; Meli, A. *Inorg. Chem.* **1984**, *23*, 2838. (e) Bianchini, C.; Mealli, C.; Meli, A.; Orlandini, A.; Saconi, L. *Inorg. Chem.* **1980**, *19*, 2968.

(40) (a) Janser, P.; Venanzi, L. M. *J. Organomet. Chem.* **1985**, *296*, 229. (b) Bianchini, C.; Meli, A.; Laschi, F.; Vacca, A.; Zanello, P. *J. Am. Chem. Soc.* **1988**, *110*, 3913. (c) Johnston, G. G.; Baird, M. C. *Organometallics* **1989**, *8*, 1894.

Scheme 7. Synthesis of **12**(BCl_4)

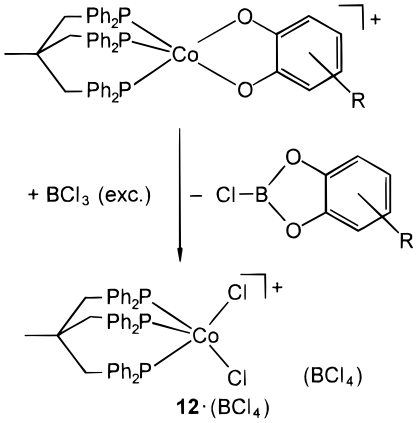

12·(BCl_4)

Table 8. Selected Bond Lengths (Å) and Angles (deg) for **11** and **12**(BCl_4)

	11	**12**(BCl_4)
Co1−P1	2.244(2)	2.185(2)
Co1−P2	2.244(2)	2.169(2)
Co1−P3	2.239(3)	2.281(2)
Co1−Cl1	2.224(3)	2.233(2)
Co1−Cl2		2.209(2)
P1−Co1−P2	91.22(9)	91.41(6)
P1−Co1−P3	89.55(9)	90.93(6)
P2−Co1−P3	93.03(9)	89.23(6)
P1−Co1−Cl1	122.9(1)	87.51(7)
P1−Co1−Cl2	122.6(1)	139.61(7)
P2−Co1−Cl1	127.5(1)	95.04(7)
P2−Co1−Cl2		128.97(7)
P3−Co1−Cl1		175.49(7)
P3−Co1−Cl2		90.29(7)
Cl1−Co1−Cl2		88.17(8)

spectra show all signals of the triphos ligand at expected positions (see Experimental Section). The cyclic voltammogram is practically identical to that of **3** (Figure 10, Experimental Section) except for the fact that the process at 340 mV in the case of $\mathbf{12}^+$ corresponds to a reduction (as confirmed by polarography). The UV/vis spectrum shows bands at 436 and around 640 nm attributable to charge-transfer and ligand-field transitions, respectively.

The five-coordinate geometry around the Co^{III} center—as deduced from the CV experiments (vide supra)—is confirmed by X-ray structural analysis results (shown in Figure 12). The metal is surrounded by three phosphorus atoms of the triphos ligand and two chloride ions in a distorted TBP geometry with P3 and Cl1 occupying axial coordination sites (Figure 12, Table 8). The distances between the metal and the axial ligands are larger than the corresponding distances of the equatorial ones (Co−P_{ax} 2.28 Å, Co−P_{eq} 2.17/2.19 Å; Co−Cl_{ax} 2.23 Å, Co−Cl_{eq} 2.21 Å, Table 8). Other [(triphos)Co^{III}] complexes found in the literature which have bidentate coligands coordinated to the cobalt ion throughout adopt a distorted SP geometry with a short Co−P_{ax} bond length (2.17−2.21 Å) and larger Co−P_{eq} lengths (2.21−2.25 Å)[1de,7,41] or a highly distorted structure intermediate between TBP and SP.[1f] The complex cation $\mathbf{12}^+$ appears to be the first example of a singlet d^6 ML_5 complex with a distorted TBP structure in the solid state. As the e′ orbital set in ideal D_{3h} symmetry is degenerate and only half-filled in the d^6 case a typical first order Jahn−Teller situation arises which favours the SP (C_{4v}) geometry or the decrease of an L−M−L angle within the trigonal plane below 80°.[42] Therefore in D_{3h} symmetry a triplet situation is usually encountered as found in $Co(PR_3)_2X_3$ (R = Me, Et; X = halide) complexes[9a,b,26] and a Co^{III} chloride complex with a tetraaza-macrocyclic ligand[9c] which have the expected $(d_{xz})^2(d_{yz})^2(d_{x^2-y^2})^1(d_{xy})^1$ electron configuation.[42] However, a diamagnetic ground state below 50 K is detected for the Co^{III} complex with the tetraaza-macrocylic ligand.[9c] Steric constraints imposed by the triphos ligand also cannot account for the geometry found in $\mathbf{12}^+$ as distortions toward the SP structure in $[(triphos)ML_2]^{n+}$ complexes are in principle possible.[1,7,14,28,41] At present we have no rational explanation for this behavior. Interestingly, the geometry (the P−Co−P and P−Co−Cl angles) found in $\mathbf{12}^+$ is very similar to the one observed in **3**, the average angular deviation being only 3.5° (calculated as the root mean square, RMS[43]) (Tables 5 and 8). The Co−P and Co−Cl distances in $\mathbf{12}^+$ (except for the Co−P3 distance) are significantly shorter than those in **3**, a fact which is certainly due to the loss of one electron in $\mathbf{12}^+$ (d^6) compared to **3** (d^7).

Conclusions

In summary, we have shown a conclusive interpretation of the peculiar solution behavior of mixtures of triphos and $CoCl_2$ originating from (i) phosphane arm-off reactions yielding the reactive high-spin complex [(η^2-triphos)$CoCl_2$] and (ii) chloride ion dissociations leading via an unsaturated intermediate [(triphos)CoCl]$^+$ to the dinuclear species [(triphos)Co(μ-Cl)$_2$Co(triphos)]$^{2+}$ and the mixed-ligand complexes [(triphos)CoCl(L)]$^+$. The [(triphos)Co^{II}Cl]$^+$ fragment as well as its reduced and oxidized analogues, [(triphos)Co^{I}Cl] and [(triphos)$Co^{III}Cl_2$]$^+$, respectively, might serve as stabilizing templates for otherwise unstable molecules—a feature well-known in the chemistry of the parent template [(triphos)Co^{II}]$^{2+}$ [44]—and as starting materials for [(triphos)Co^{I}] and [(triphos)Co^{III}] complexes, respectively. This is the subject of current investigations.

Acknowledgment. This work received support from the Deutsche Forschungsgemeinschaft, the Fonds der Chemischen Industrie and the Volkswagenstiftung.

Supporting Information Available: Tables listing crystallographic data for details of the structure determinations of **1**(BPh_4)$_2$, **3**, **4**, **1**(Zn_2Cl_6), **1**($CoCl_3THF$)$_2$, **5**, **6**, **8**(BPh_4), **9**(BPh_4), **10**(BPh_4), **11**, and **12**(BCl_4) and figures showing the cations of **1**(BPh_4)$_2$, **1**(Zn_2Cl_6), **1**($CoCl_3THF$)$_2$, and **3** and the cation of **12**(BCl_4), $-R\ln(K)$ vs T^{-1} plots and molar high-spin fraction vs T plots for the **2**/**3** equilibrium, details of the dilution and titration studies, molar magnetic susceptibility vs T plots for **1**(Zn_2Cl_6), **3**, **5**, and **6**, and electronic spectra of **2** and **4** in THF (47 pages). Ordering information is given on any current masthead page.

IC9705352

(41) Körner, V.; Vogel, S.; Huttner, G.; Zsolnai, L.; Walter, O. *Chem. Ber.* **1996**, *129*, 1107.

(42) (a) Rossi, A. R.; Hoffmann, R. *Inorg. Chem.* **1975**, *14*, 365. (b) Jean, Y.; Eisenstein, O. *Polyhedron*, **1988**, *7*, 405. (c) Rachidi, I. E.-I.; Eisenstein, O.; Jean, Y. *New J. Chem.* **1990**, *14*, 671. (d) Riehl, J.-F.; Jean, Y.; Eisenstein, O.; Pélissier, M. *Organometallics* **1992**, *11*, 729.

(43) The root mean square is defined as: RMS = $\{(1/n\sum_{i=1}^{n}[\alpha_i(\mathbf{3}) - \alpha_i(\mathbf{13}^+)]^2\}^{1/2}$, where α_i = P−Co−P, P−Co−Cl, and Cl−Co−Cl angles and n = 10.

(44) (a) Vogel, S.; Barth, A.; Huttner, G.; Klein, T.; Zsolnai, L.; Kremer, R. *Angew. Chem.* **1991**, *103*, 325; *Angew. Chem., Int. Ed. Engl.* **1991**, *30*, 303. (b) Bianchini, C.; Meli, A. *J. Chem. Soc., Chem. Commun.* **1983**, 156. (c) Bianchini, C.; Meli, A.; Orlandini, A. *Angew. Chem. Suppl.* **1982**, 471. (d) Di Vaira, M.; Ghilardi, C. A.; Midollini, S.; Sacconi, L. *J. Am. Chem. Soc.* **1978**, *100*, 2550. (e) Bianchini, C.; Di Vaira, M.; Meli, A.; Sacconi, L. *Inorg. Chem.* **1981**, *20*, 1169. (f) Capozzi, G.; Chiti, L.; Di Vaira, M.; Peruzzini, M.; Stoppioni, P. *J. Chem. Soc., Chem. Commun.* **1986**, 1799. (g) Di Vaira, M.; Midollini, S.; Sacconi, L. *J. Am. Chem. Soc.* **1979**, *101*, 1757. (h) Di Vaira, M.; Peruzzini, M.; Stoppioni, P. *J. Chem. Soc., Dalton Trans.* **1984**, 359. (i) Barth, A.; Huttner, G.; Fritz, M.; Zsolnai, L. *Angew. Chem.* **1990**, *102*, 956; *Angew. Chem., Int. Ed. Engl.* **1990**, *29*, 929.

(45) The phenyl groups of the triphos ligand and all hydrogens have been omitted for the sake of clarity. The thermal ellipsoids are drawn at the 70% probability level. A numbering scheme identical for all complexes is used for the sake of easier comparison, unlike the numbering schemes of the deposited structures. Zsolnai, L.; Huttner, G. XPMA, ZORTEP, University of Heidelberg, 1997.